LHC Project Note 251
4 April 2001
Claire.Fynbo@cern.ch
Graham.Stevenson@cern.ch

Compendium of annual doses in the LHC arcs

Author(s) / EST-LEA: Claire A. Fynbo, TIS: Graham R. Stevenson

Keywords: annual doses, LHC arcs

Summary:

This report presents dose maps in and around the standard arc magnet cell due to beam-gas interactions, for nominal LHC running conditions. These maps update and confirm previous dose values expected in the LHC tunnel, and also present expected doses to internal magnet components.

1. Introduction

The aim of this study of the LHC arc sections is to provide estimations of the annual dose to the standard arc machine components due to the secondary particle cascades originating from inelastic interactions of the circulating 7 TeV proton beams with the small amount of residual gas present in the vacuum chamber of the collider. Values of $1.65 \times 10^{11} \mathrm{m}^{-1} \mathrm{y}^{-1}$ ($1.05 \times 10^{4} \mathrm{m}^{-1} \mathrm{s}^{-1}$) for the proton losses due to beam-gas interactions, calculated for the so-called 'Design Machine', are to be found in [Pot95a], [Pot95b]. Previous studies have provided dose estimations in and around the machine cryostat extending to the tunnel wall [Pot95b], [Huh96], [Ama99] & [Fyn00]. This study confirms previous reported doses at the tunnel walls of a few Gray per year opposite the magnet string for the majority of the arc cell, with a few regions in the vicinity of the quadrupole and the inter-magnet gaps reaching values of a few tens of Gray. This study also provides expected doses to the inner components of the arc magnets *e.g.* magnet coils, collars, yokes, plastic filler pieces etc. The hadronic cascade simulations were performed using the Monte-Carlo particle shower code FLUKA[Fas93], [Fas94], [Fas97a], [Fas97b], [Fer96] using as full and accurate description of the arc's main dipole (MB) and quadrupole (MQ) magnets as possible.

For the dose expected in other sections of the LHC machine see [Ste00] and references therein.

2. FLUKA simulation of the LHC standard arc section

The full FLUKA geometry for the LHC arc section consisting of six main bending dipole magnets (MBA

/MBB), the quadrupole (MQ) and their correcting magnets is shown in Figure 1. The geometry is setup according to LHC design optics 6.2 (which for the arcs remains unchanged for the upcoming new optics version 6.3).

To simulate the radiation environment of the LHC arcs, 7 TeV proton beams were sent down each of the two beam pipes and interaction of the incident protons forced every 2 metres along the entire geometry. For each longitudinal position of the interaction point a separate simulation run is required. Energy depostion was scored in various sized meshes covering the entire geometry: $2 \times 2 \times 50\,\mathrm{cm}^3$ mesh bins were used in the central regions of the magnets to provide detailed dose maps in the coil and collar sections; bins of $5 \times 5 \times 50\,\mathrm{cm}^3$ were used to cover the magnet yokes and cryostat regions and bins of size $20 \times 20 \times 50\,\mathrm{cm}^3$ were used to score dose in the air of the tunnel, tunnel walls and floor. The final energy deposition in each mesh bin is the total of all contributions arising from each of the interaction point runs. Total energy deposition (GeV) is then converted to Dose (1 Gy=1 J/Kg) and normalized using the given proton loss per year ($1.65 \times 10^{11}\mathrm{m}^{-1}\mathrm{y}^{-1}$) - giving annual dose per year in each scoring bin. Due to the large proportion of neutrons produced by interactions within the magnet material surrounding the beam pipes, dose estimations are sensitive to the type of material used to score energy deposition [Huh96], *i.e.* dose scored in a hydrogenous material such as polythene can be as much as twice the dose scored in an inorganic material such as aluminium or air. Thus, this simulation uses the correct material for each magnet component wherever possible to provide the most accurate dose estimation for the different sections in the magnets.

Various dose maps for the LHC arc sections are to be found in the remainder of this report covering a selection of different longitudinal and cross-sectional cuts. Specific details for each cut can be found with the relevant Figure. Details for a specific longitudinal position in the arc section are known to 50 cm (longitudinal dimension of scoring bin). Note, in this simulation, since interactions are only considered in the length of the geometry shown, then contributions to the dose at each end of the FLUKA arc section arising from interactions upstream of the ends of the geometry are not taken into consideration. Thus, for figures showing the full length of the arc geometry, doses in the end regions of the external dipole magnets should be ignored (reliable doses can be taken to start from approximately the middle of the outer dipoles). A comprehensive list of the available figures appears after the Reference section. For cuts not appearing in this compendium, please use the contact details in this report.

References

[Ama99] J. F. Amand, Presentation given October 1999 at private meeting on *Radiation dose calculations in the LHC tunnel*, CERN (unpublished).

[Fas93] A. Fassò, A. Ferrari, J. Ranft and P. R. Sala, *FLUKA: present status and future developments*, Proc IV Int. Conf. on Calorimetry in High Energy Physics, La Biodola (Isola d'Elba), Sept. 20-25 1993. Ed. A. Menzione and A. Scribano, World Scientific, p. 493 (1993).

[Fas94] A. Fassò, A. Ferrari, J. Ranft and P. R. Sala, *FLUKA: Performances and Applications in the Intermediate Energy Range*, Specialists' Meeting on Shielding Aspects of Accelerators, Targets and Irradiation Facilities. Arlington, Texas, April 28-29 1994, NEA/OECD (Paris) p. 287.

[Fas97a] A. Fassò, A. Ferrari, J. Ranft and P. R. Sala, *An update about FLUKA*, Proc. 2nd Workshop on Simulating Accelerator Radiation Environments, CERN, Geneva, Switzerland 9-11 Oct. 1995, Ed. G.R. Stevenson, CERN Report TIS-RP/97-05, p.158-170.

[Fas97b] A. Fassò, A. Ferrari, J. Ranft and P. R. Sala, *New developments in FLUKA modelling hadronic and EM interactions*, Proc. 3rd Workshop on Simulating Accelerator Radiation Environments, KEK, Tsukuba, Japan 7-9 May 1997, Ed. H. Hirayama, KEK Proceedings 97-5, p.32-43.

[Fer96] A. Ferrari and P. R. Sala, *The Physics of High Energy Reactions*, in Proceedings of the Workshop on Nuclear Reaction Data and Nuclear Reactors Physics, Design and Safety, International Centre for Theoretical Physics, Miramare-Trieste, Italy, 15 April - 17 May 1996, Ed. A. Gandini and G. Reffo, World Scientific, p.424 (1998).

[Fyn00] C. A. Fynbo and G. R. Stevenson, *The ratio of doses to neutron and hadron fluences for components exposed to LHC beam-gas interactions*, EST Technical Note EST-LEA / 2000-001.

[Huh96] M. Huhtinen and G. R. Stevenson, *Doses around the LHC beam-pipe due to beam-gas interactions in a long straight section*, CERN-LHC Project Note 39 (1996).

[Pot95a] K. Potter and G. R. Stevenson, *Source intensities for use in the radiological assessment of the effect of proton losses at the scrapers and around the main ring of the LHC*, CERN Internal Report TIS–RP / IR / 95–16 (1995), CERN AC / 95–04(DI), LHC Note 322.

[Pot95b] K. Potter, H. Schönbacher and G. R. Stevenson, *Estimates of dose to components in the arcs of the LHC due to beam-loss and beam-gas interactions*, CERN-LHC Project Note 18 (1995).

[Ste00] G. R. Stevenson and C. A. Fynbo, *The LHC-machine radiation environment*, Presented at the CERN TECHNICAL TRAINING meeting on Radiation Effects on Electronic Components and Systems for LHC, held 10-12 April 2000. Can be obtained under 'CERN Courses on Radiations' under the Radiation Working Group (RADWG) web page.

List of figures:

Geometry simulation of LHC arc section
(all dimensions are in cm)

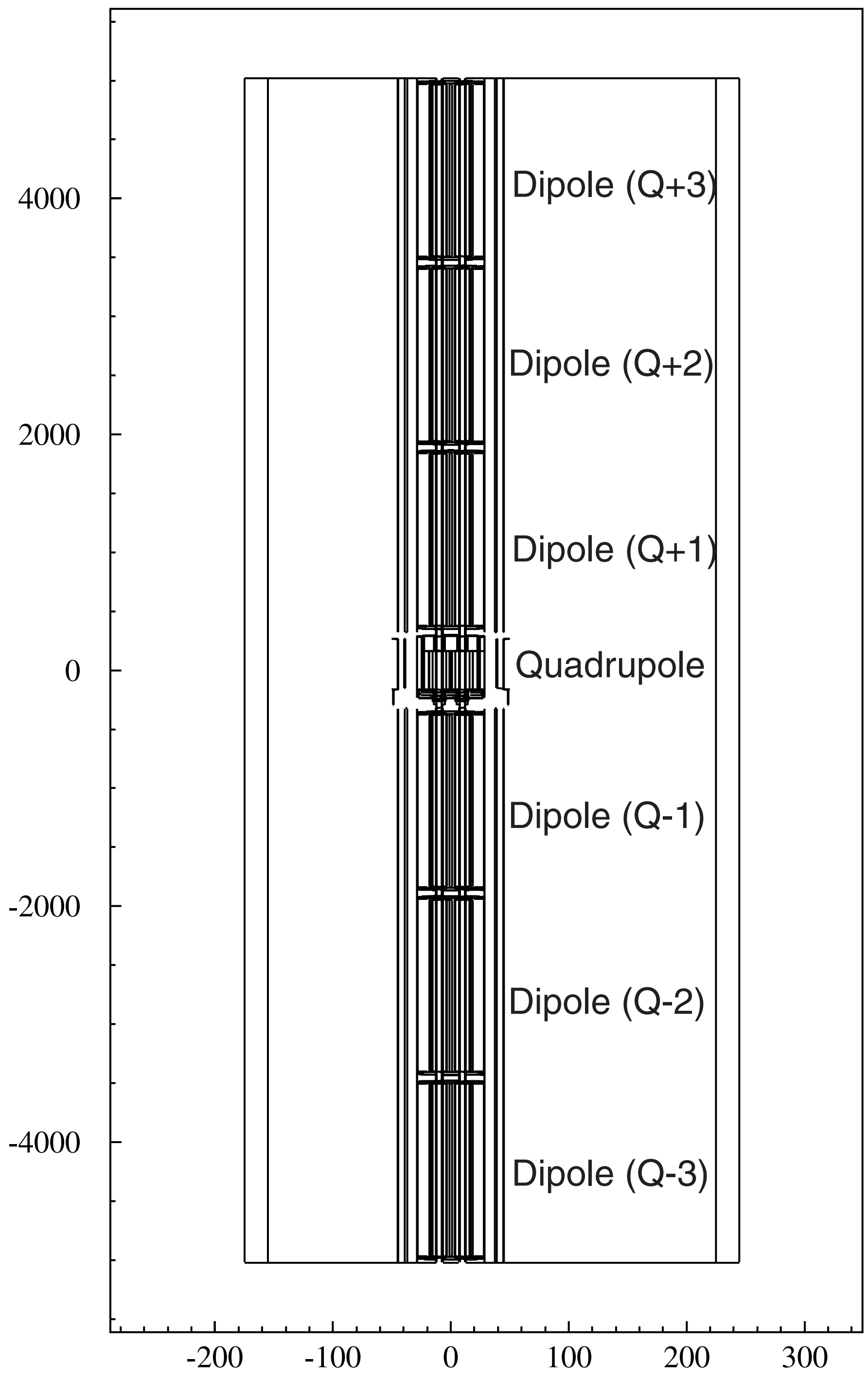

Figure 1

Full LHC arc geometry including tunnel

Annual Doses

Annual dose in the LHC standard arcs

Horizontal cut - averaged over 20cm about beam-axis
full tunnel cross-section

(for proton losses 1.65×10^{11} pm^{-1} y^{-1} for 2 beams)

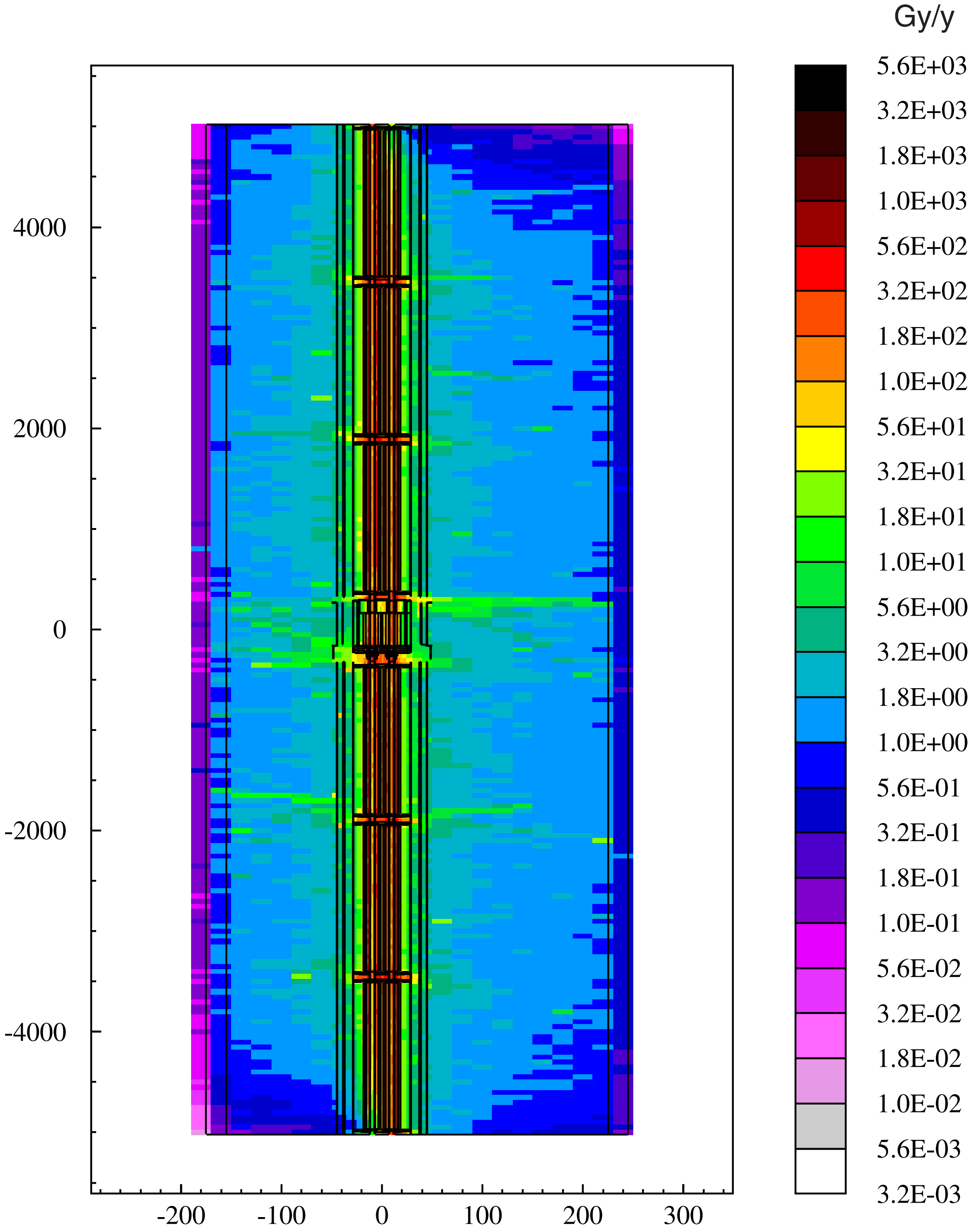

Figure 2

Annual dose in LHC arcs

Longitudinal cut - doses under main magnets
(for proton losses $1.65 \times 10^{11}\ \mathrm{pm}^{-1}\ \mathrm{y}^{-1}$ for 2 beams)

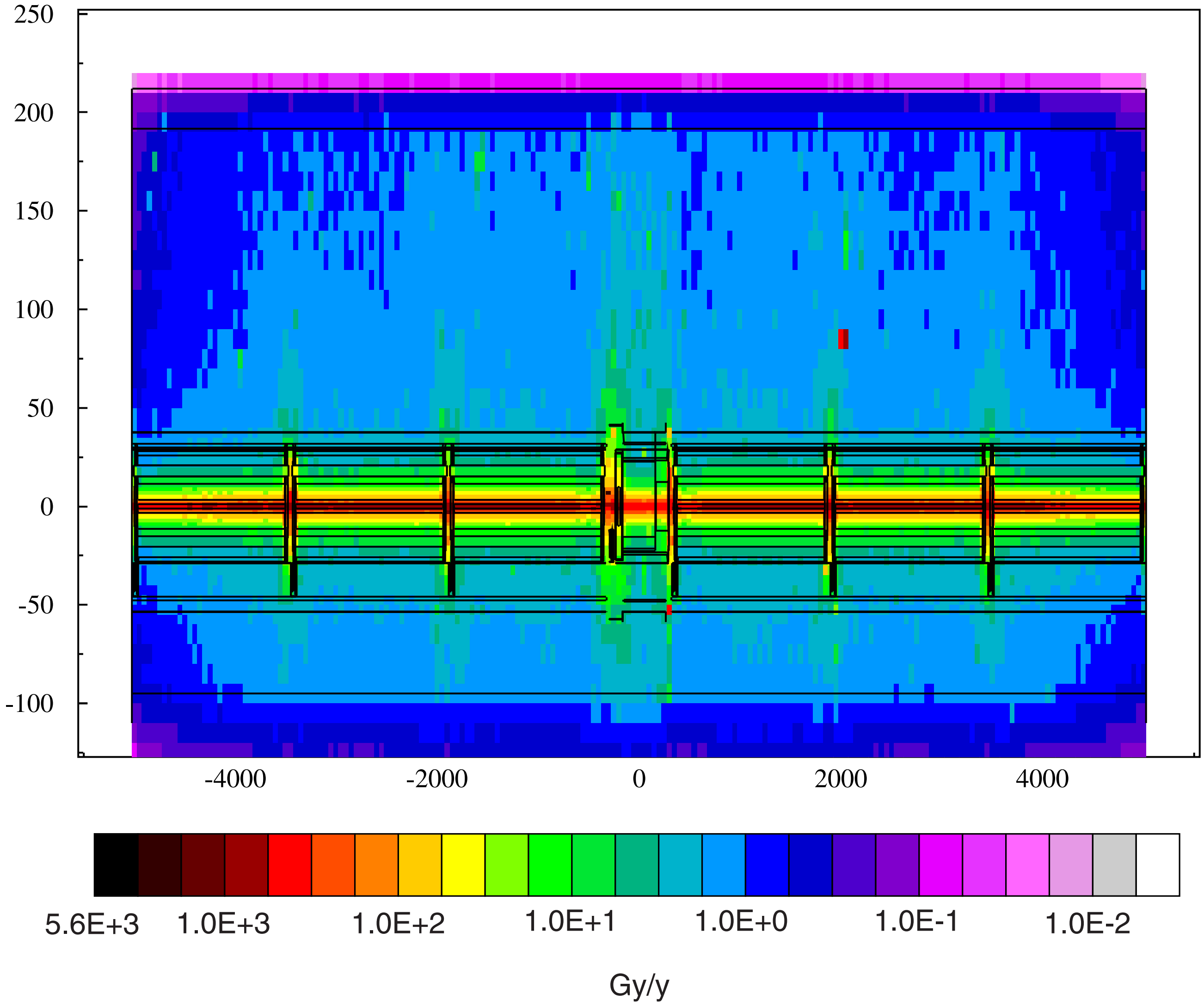

Figure 3

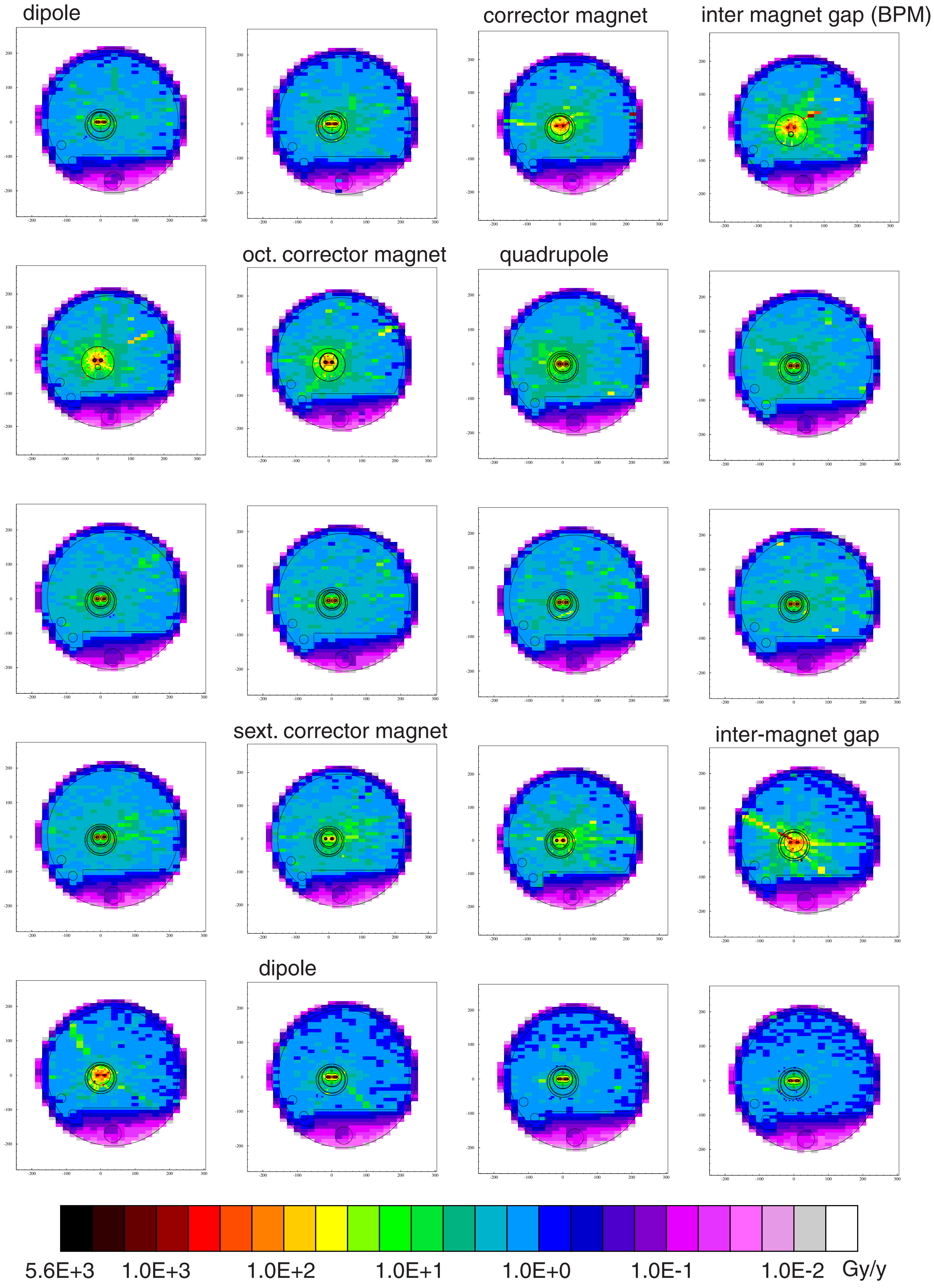

(Longitudinal cuts every 50cm)
Cross-section of tunnel in LHC Arcs - Annual doses Gy/y
Dipole - Quadrupole - Dipole region

Figure 4

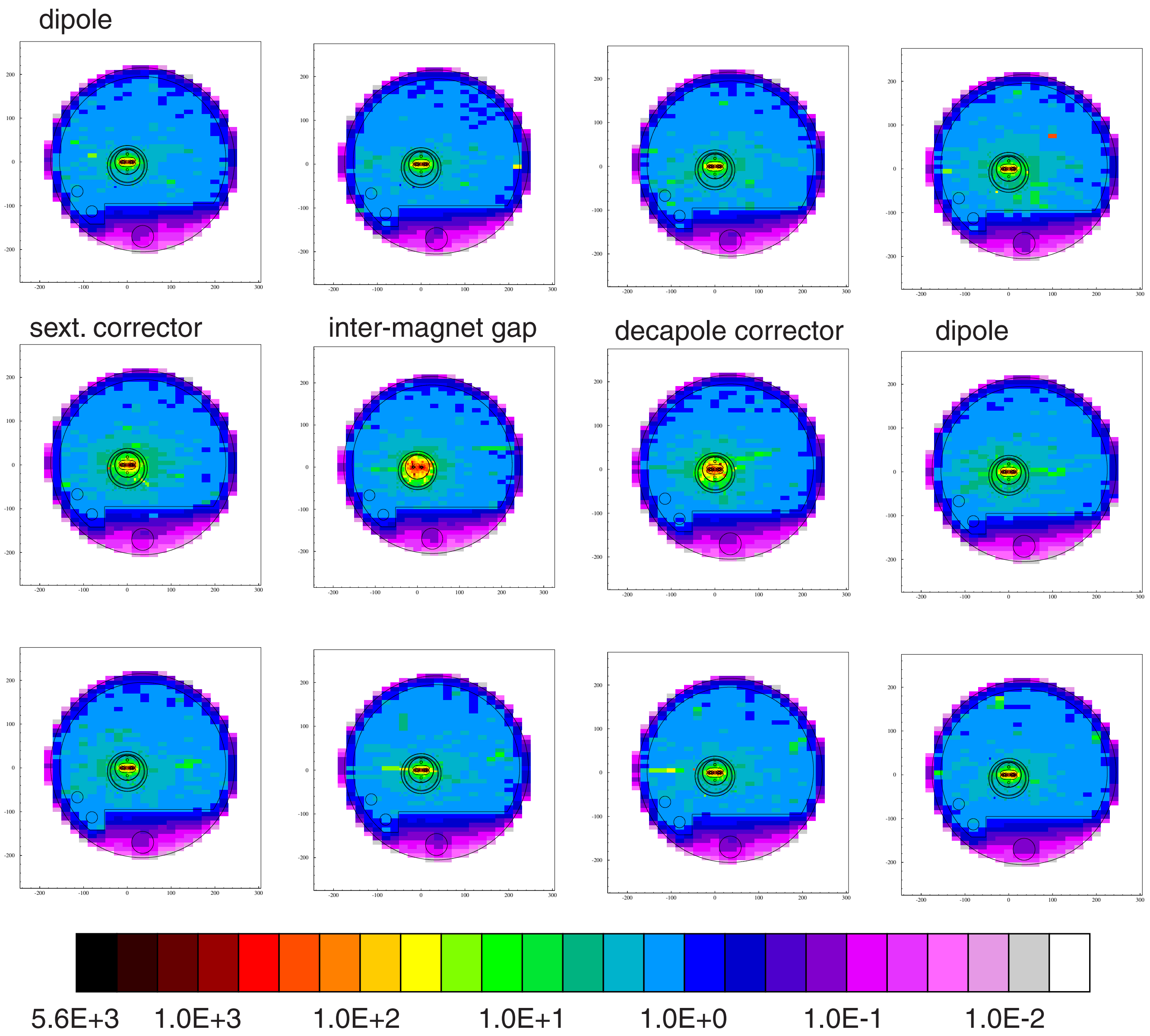

Cross-section of tunnel in LHC Arcs - Annual doses Gy/y
Dipole - Dipole region (Q-2 / Q-1)
(Longitudinal cuts every 50cm)

Figure 5

Annual dose in concrete floor of the LHC tunnel

0-5cm below the surface

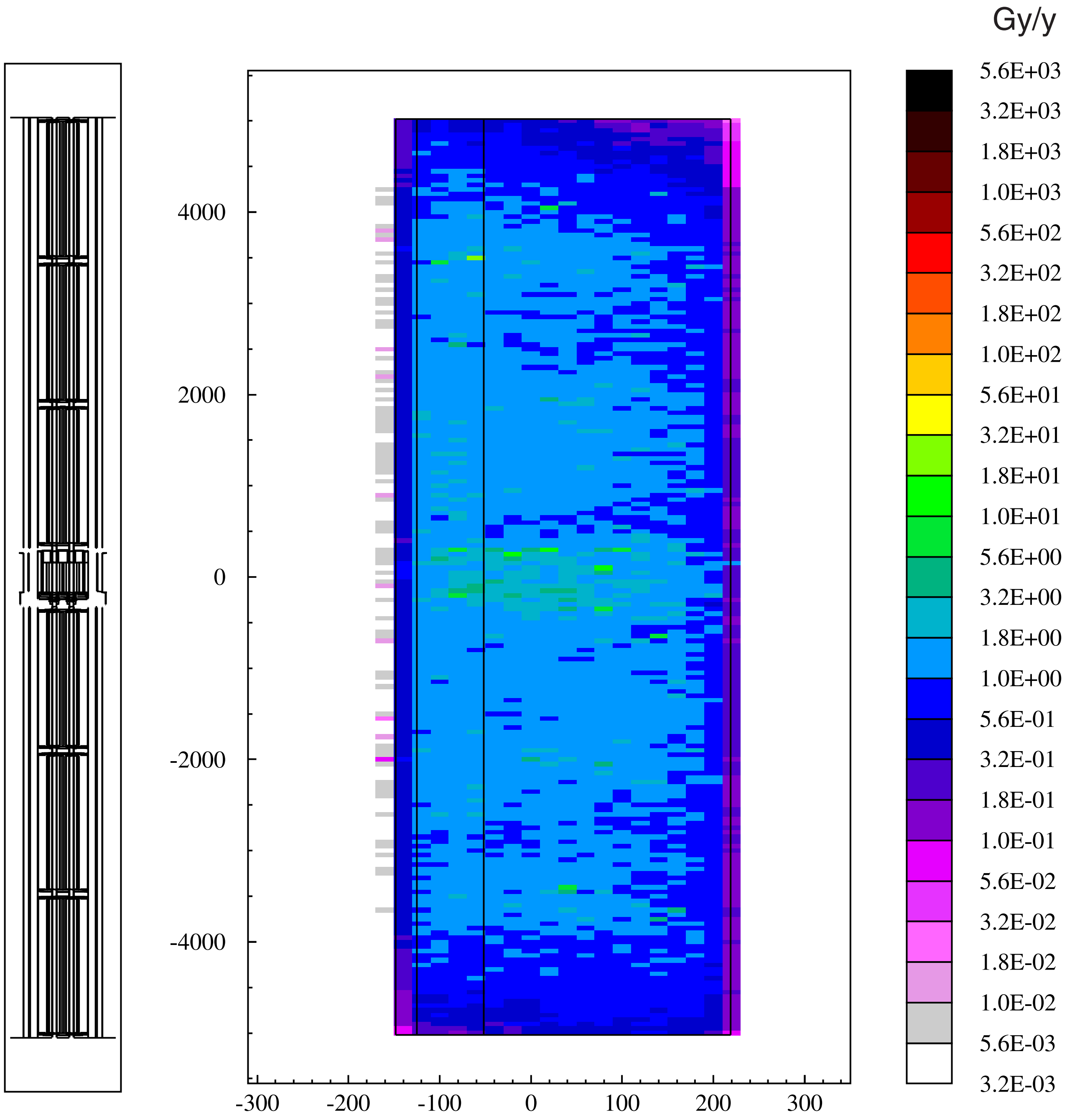

Figure 6a

Annual dose in concrete floor of the LHC tunnel

5-15cm below the surface

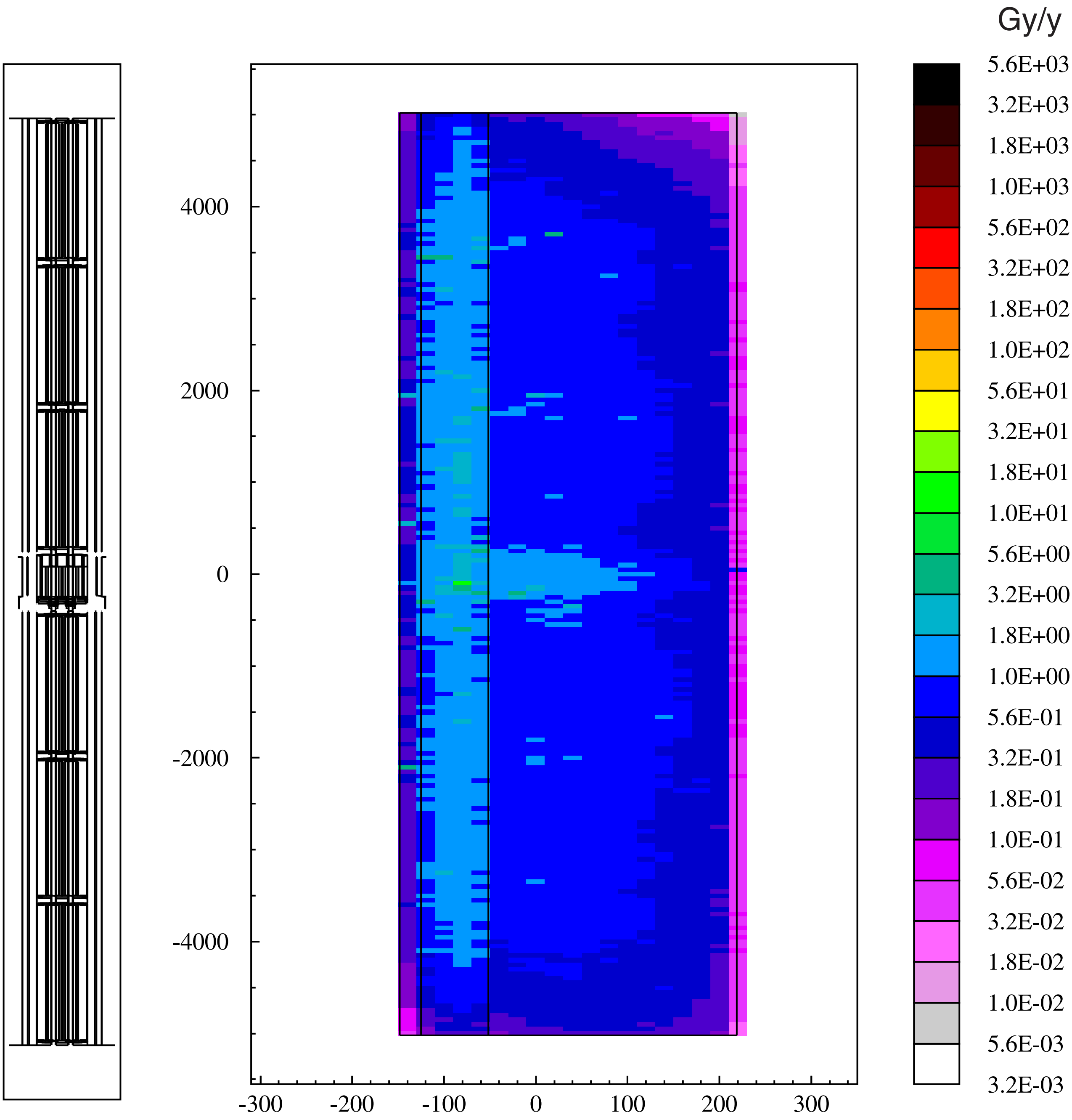

Figure 6b

Annual dose in concrete floor of the LHC tunnel

15-25cm below the surface

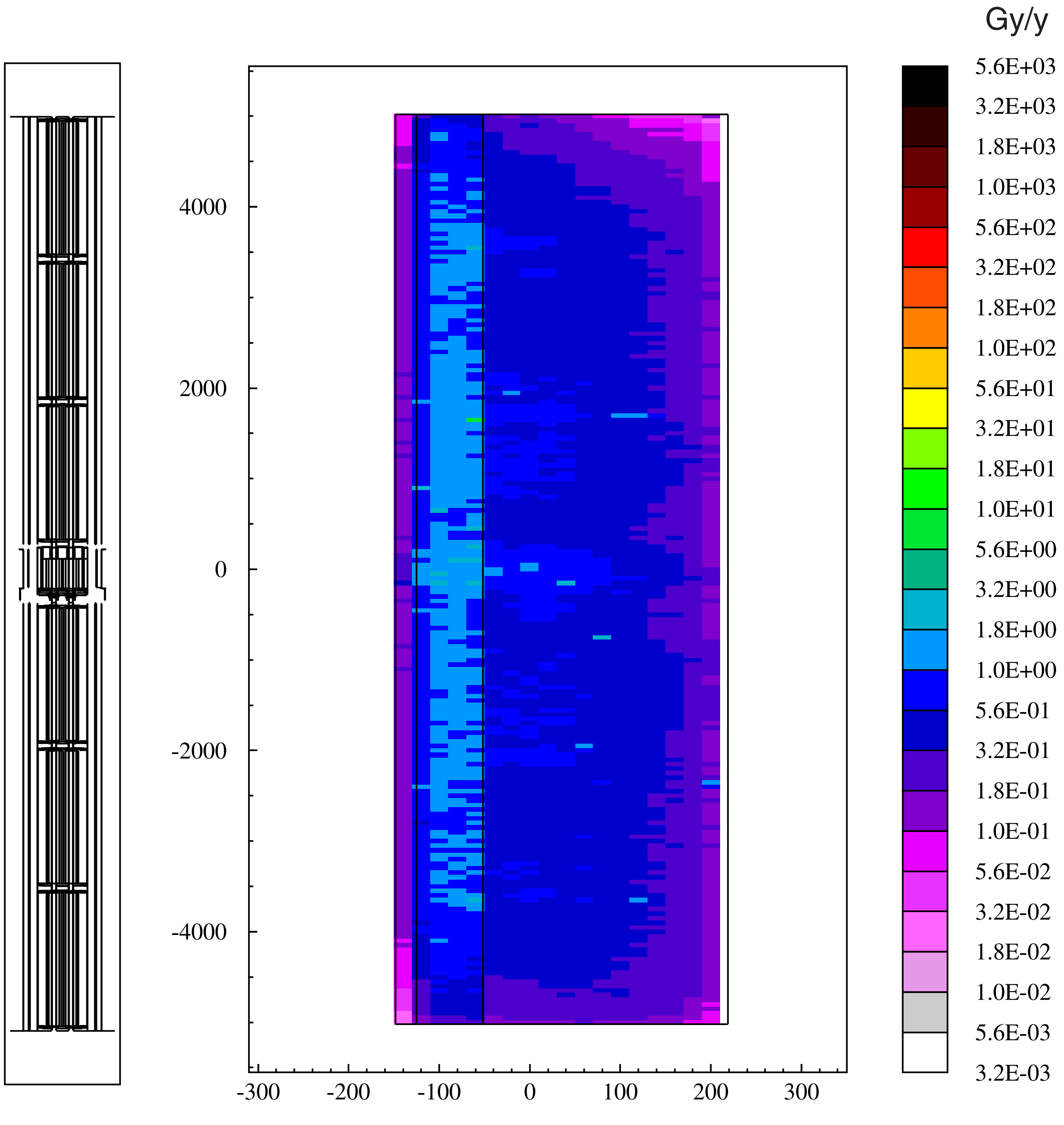

Figure 6c

Annual dose in concrete floor of the LHC tunnel

25-35cm below the surface

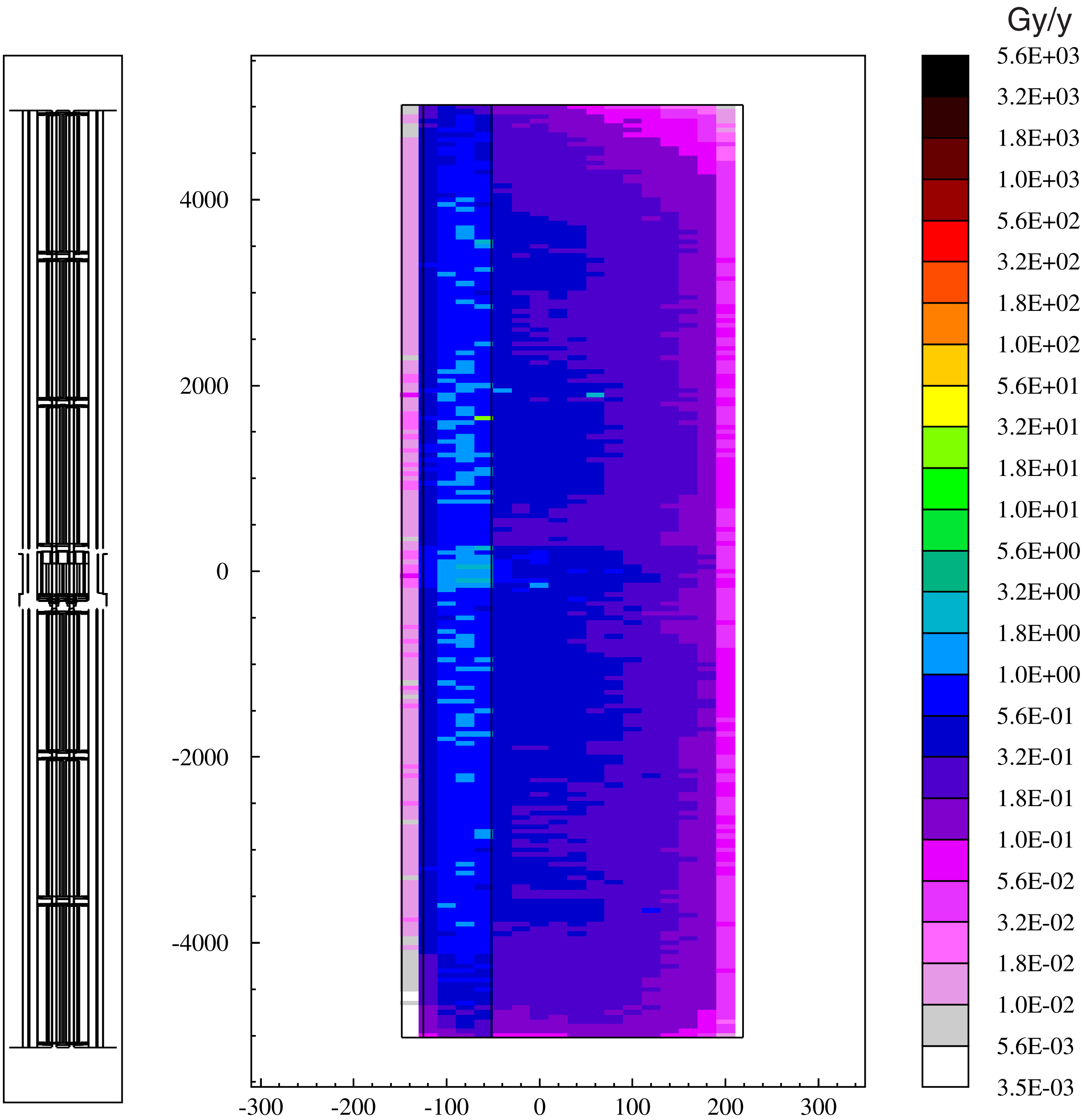

Figure 6d

Inner regions of LHC arc magnets

Dipoles

Annual dose to the inner regions of the LHC standard arcs

Horizontal cut - averaged over 20cm about beam-axis

(for proton losses $1.65x10^{11}$ pm^{-1} y^{-1} for 2 beams)

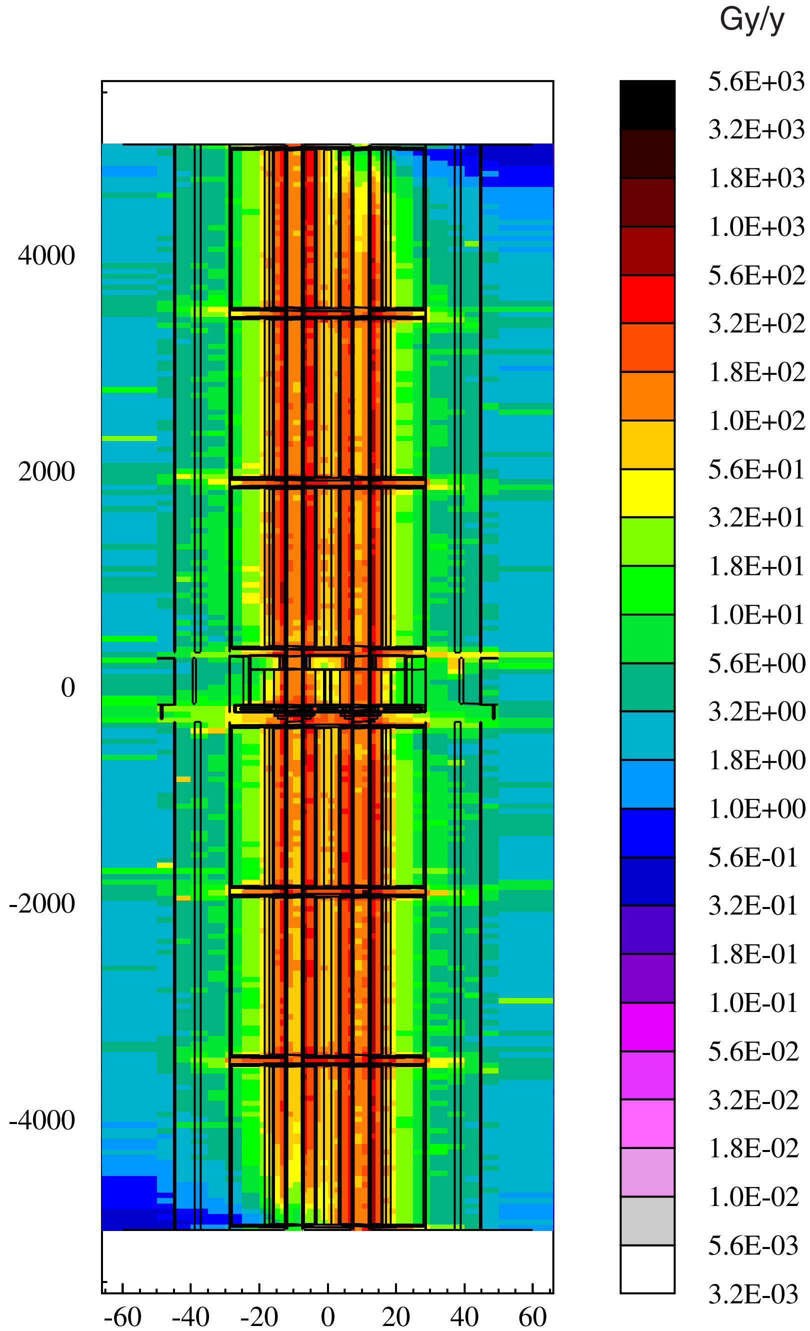

Figure 7

Annual dose to inner region of arc dipoles

(averaged over 13m of dipole coil)

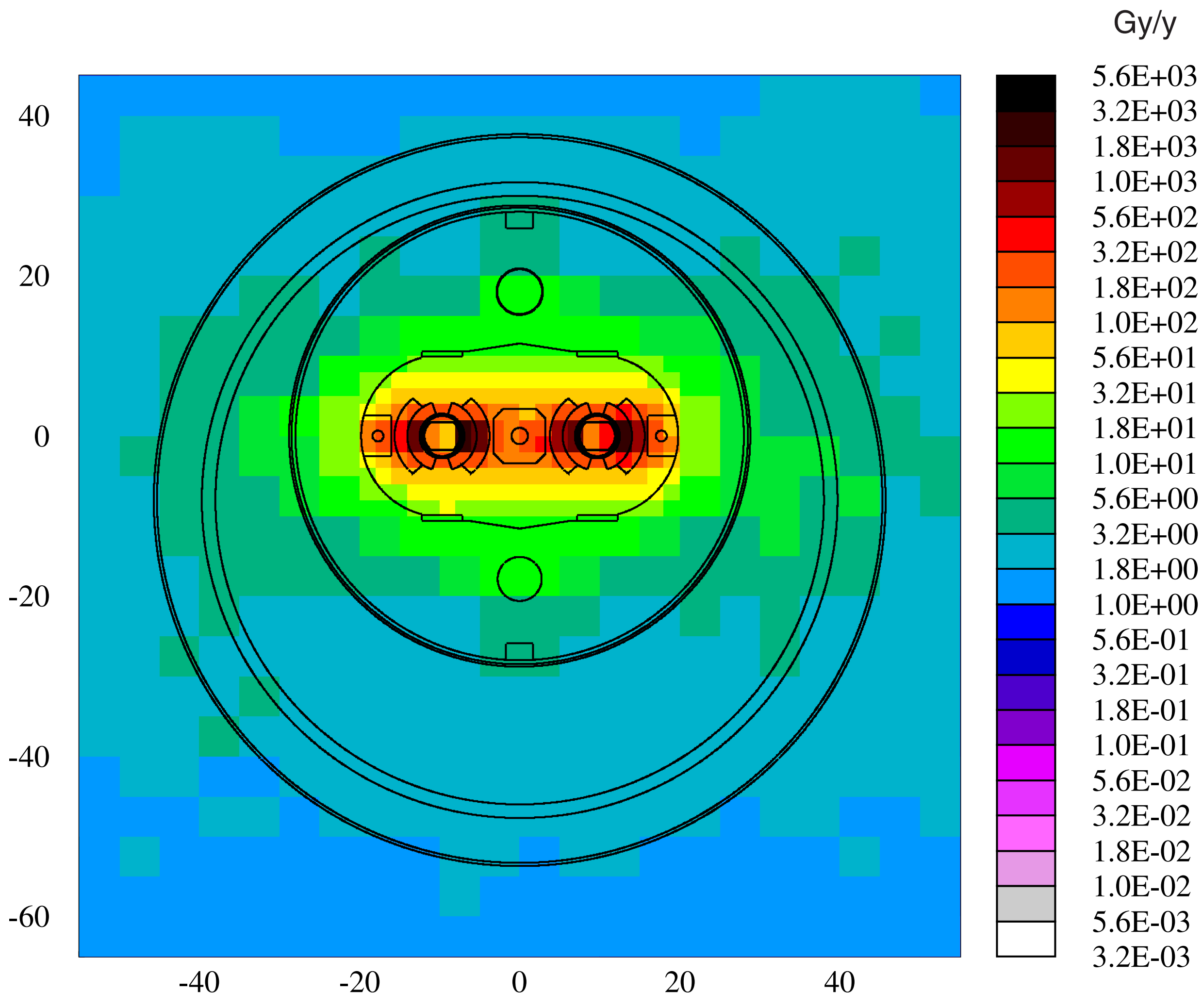

proton losses: $1.65 \times 10^{11} pm^{-1} y^{-1}$ for 2 beams

Figure 8

Annual dose to dipole end coils (Q-2)

(50cm longitudinal scoring bin - shaded)

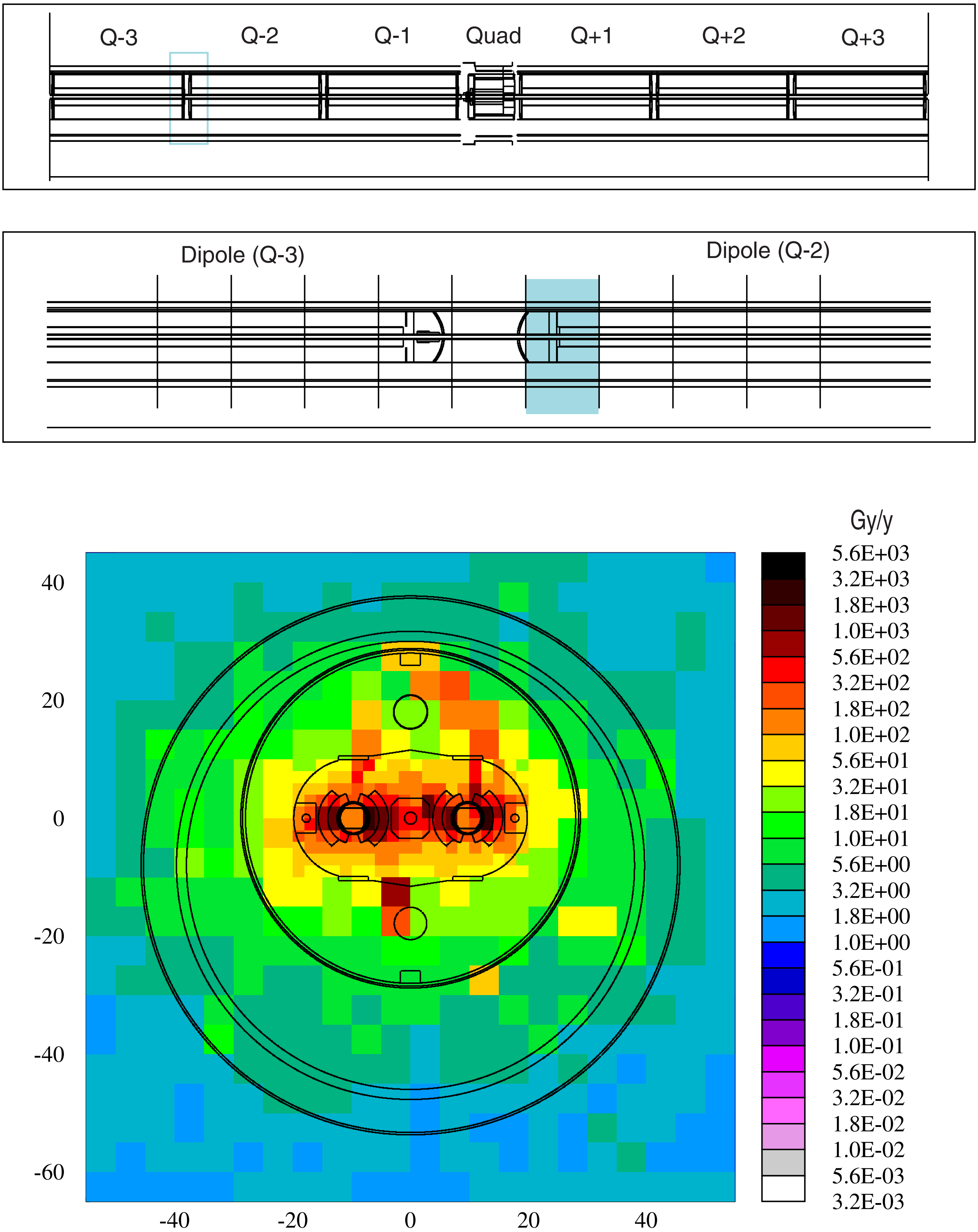

proton losses: 1.65×10^{11} pm^{-1} y^{-1} for 2 beams

Figure 9

Annual dose to MCS corrector and dipole end coils (Q-2)

(50cm longitudinal scoring bin - shaded)

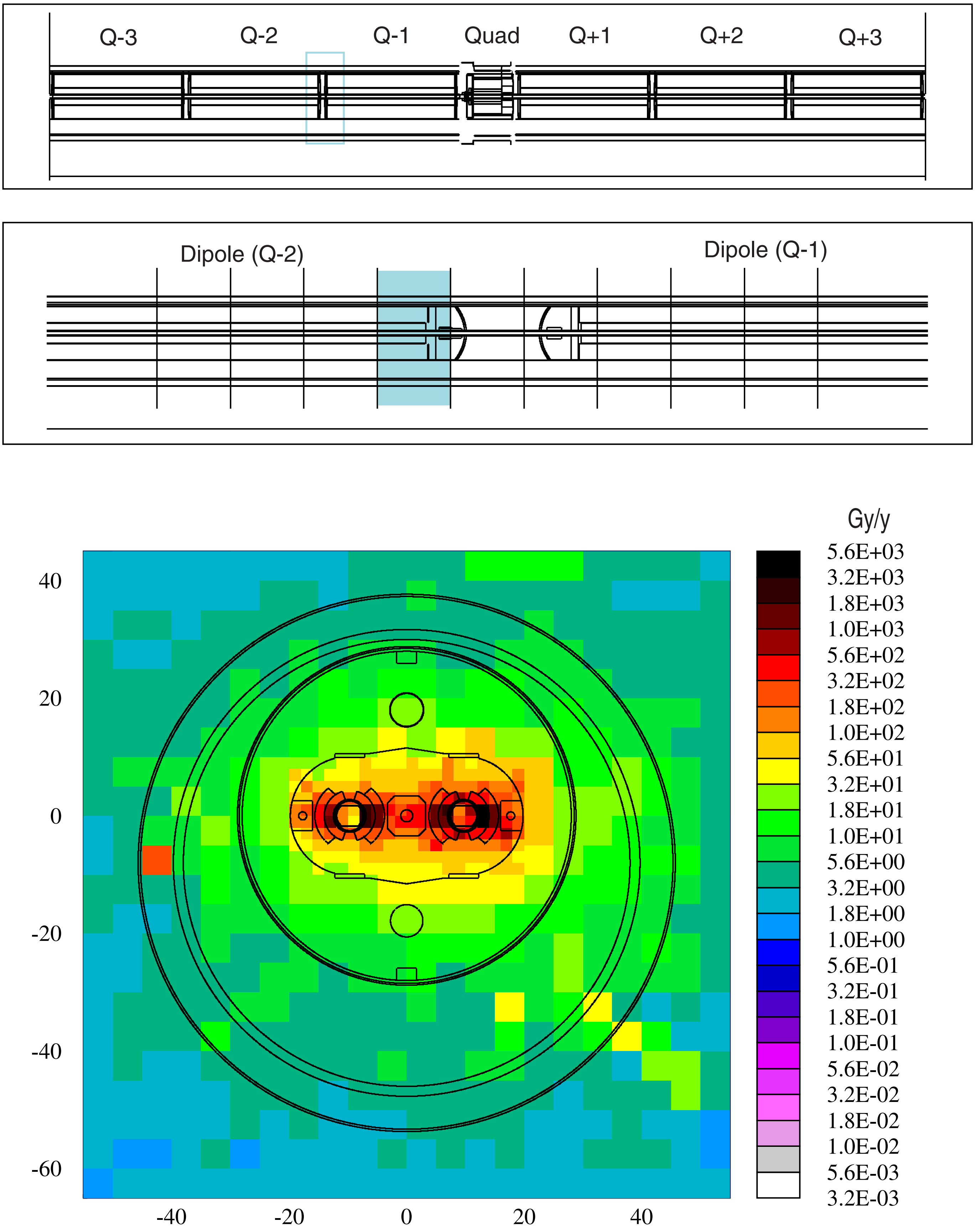

proton losses: 1.65×10^{11} pm^{-1} y^{-1} for 2 beams

Figure 10

Annual dose to decapole corrector and dipole end coils (Q-1)

(50cm longitudinal scoring bin - shaded)

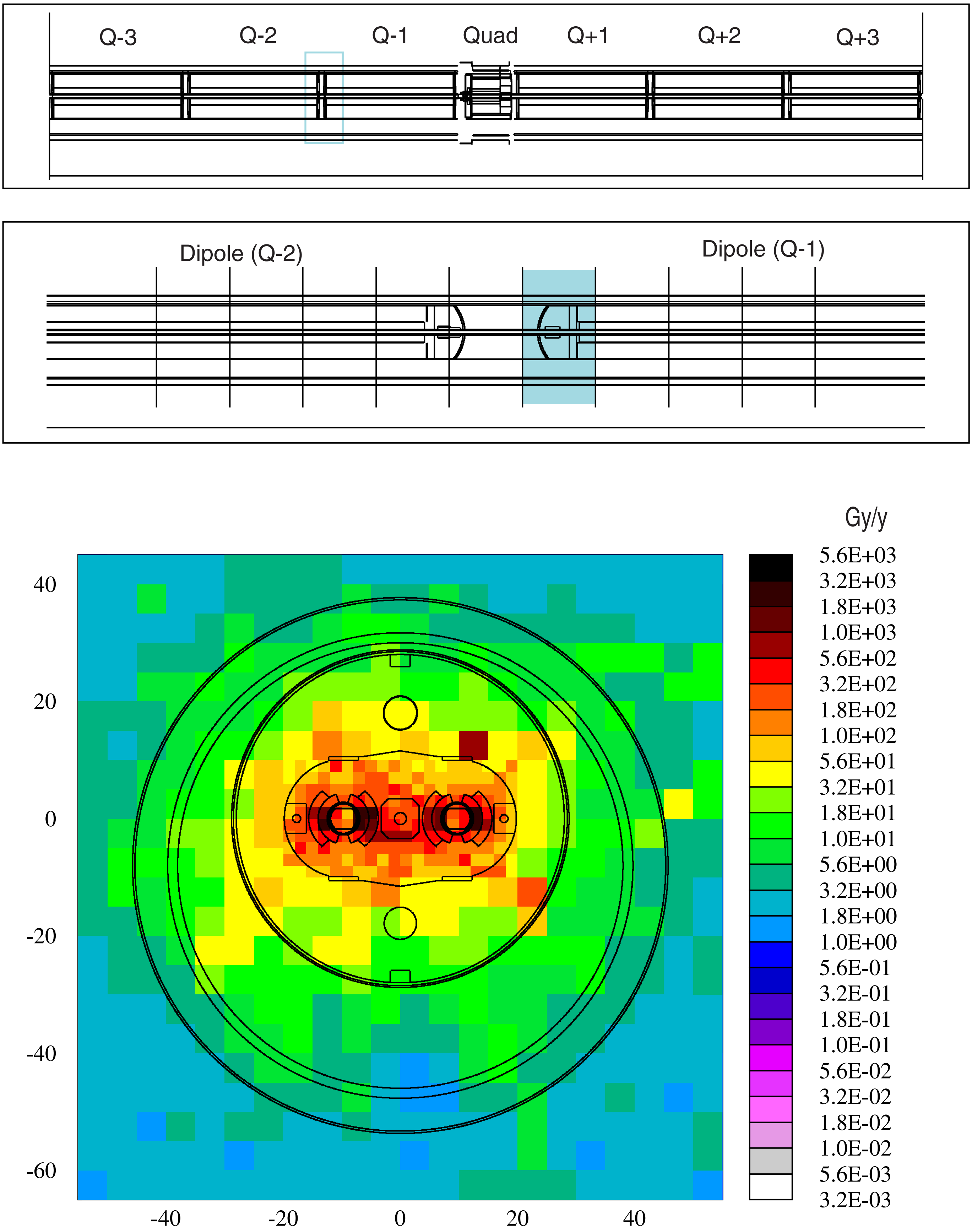

proton losses: 1.65×10^{11} pm^{-1} y^{-1} for 2 beams

Figure 11

Annual dose to dipole end coils (Q-1)

(50 cm longitudinal scoring bin - shaded)

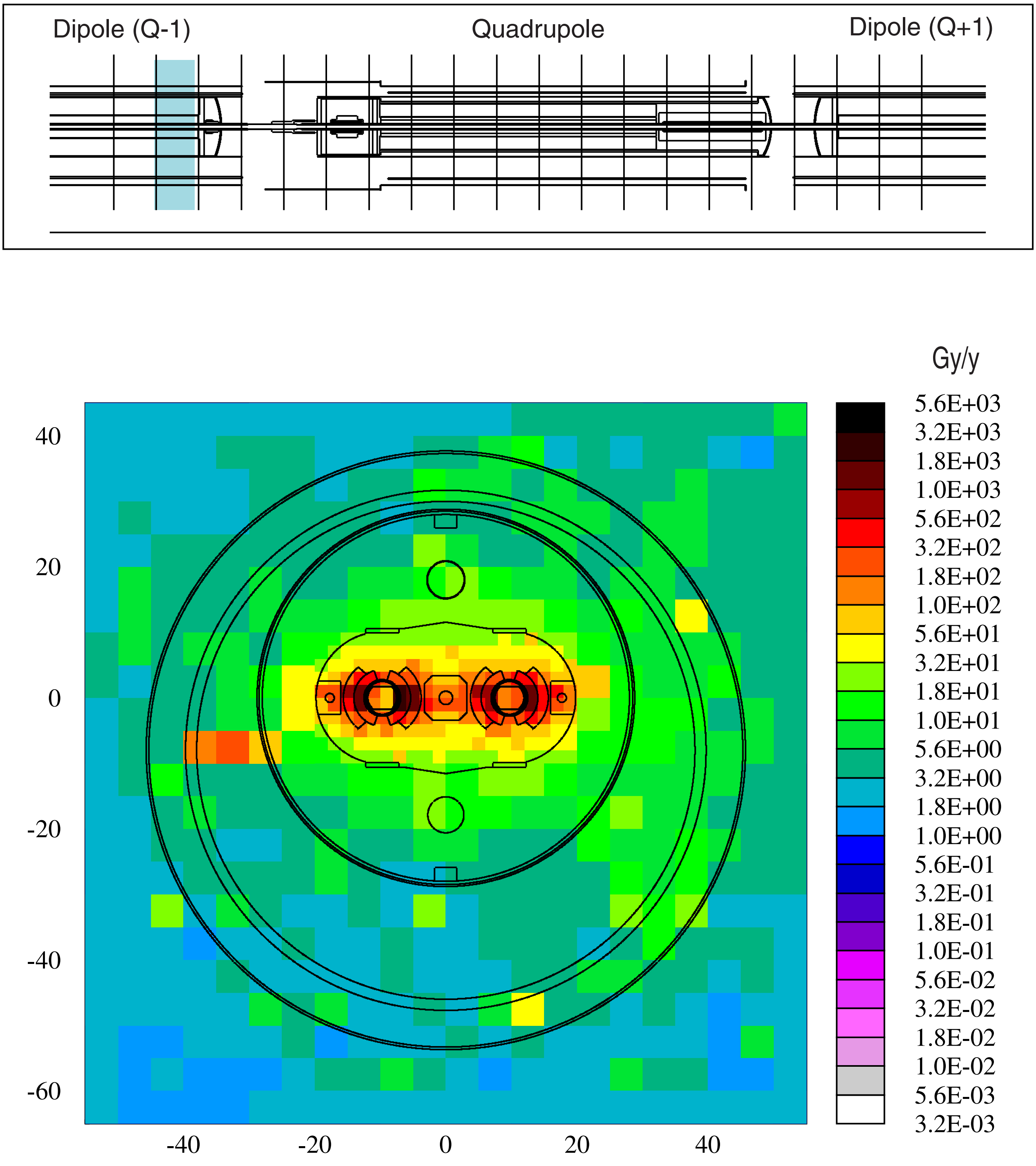

proton losses: 1.65×10^{11} pm^{-1} y^{-1} for 2 beams

Figure 12

Annual dose to sextupole corrector magnet MCS (Q-1)

(50 cm longitudinal scoring bin - shaded)

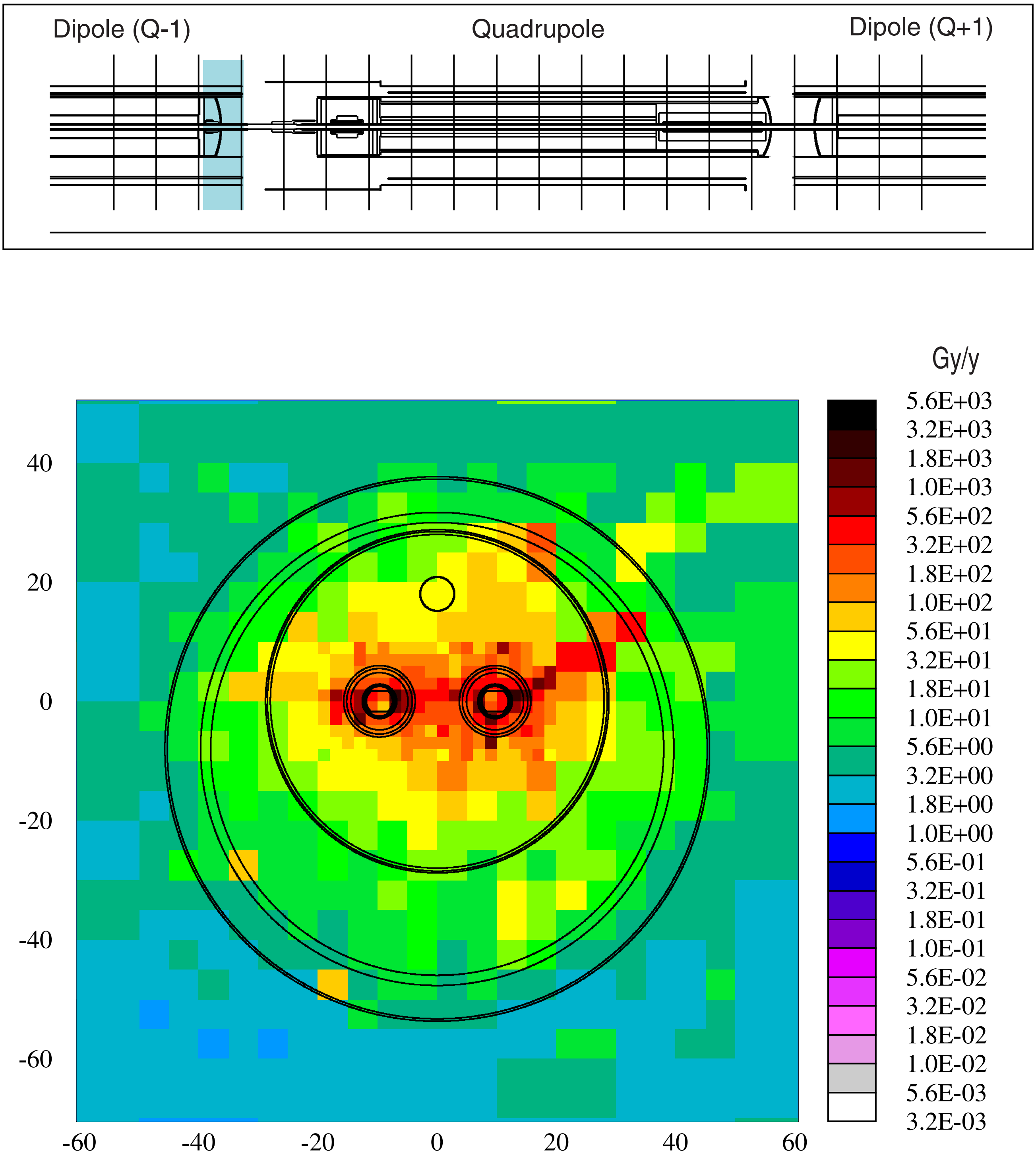

proton losses: 1.65×10^{11} pm^{-1} y^{-1} for 2 beams

Figure 13

Annual dose to dipole end coils (Q+1)

(50 cm longitudinal scoring bin - shaded)

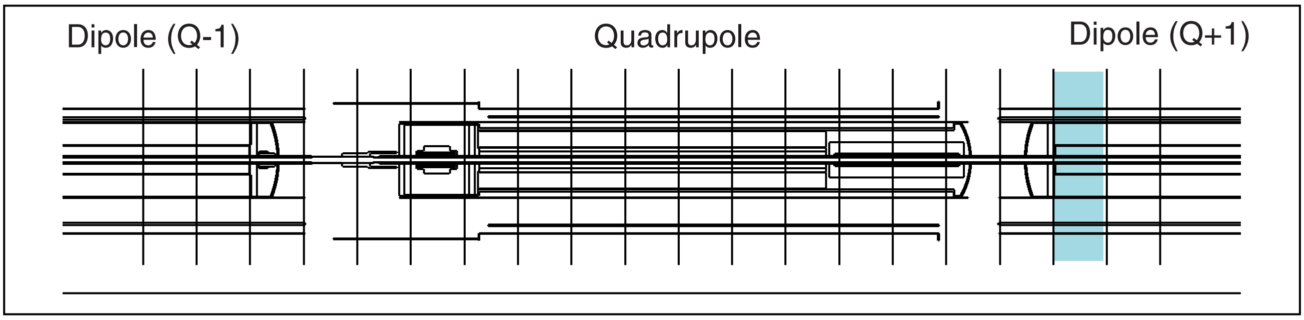

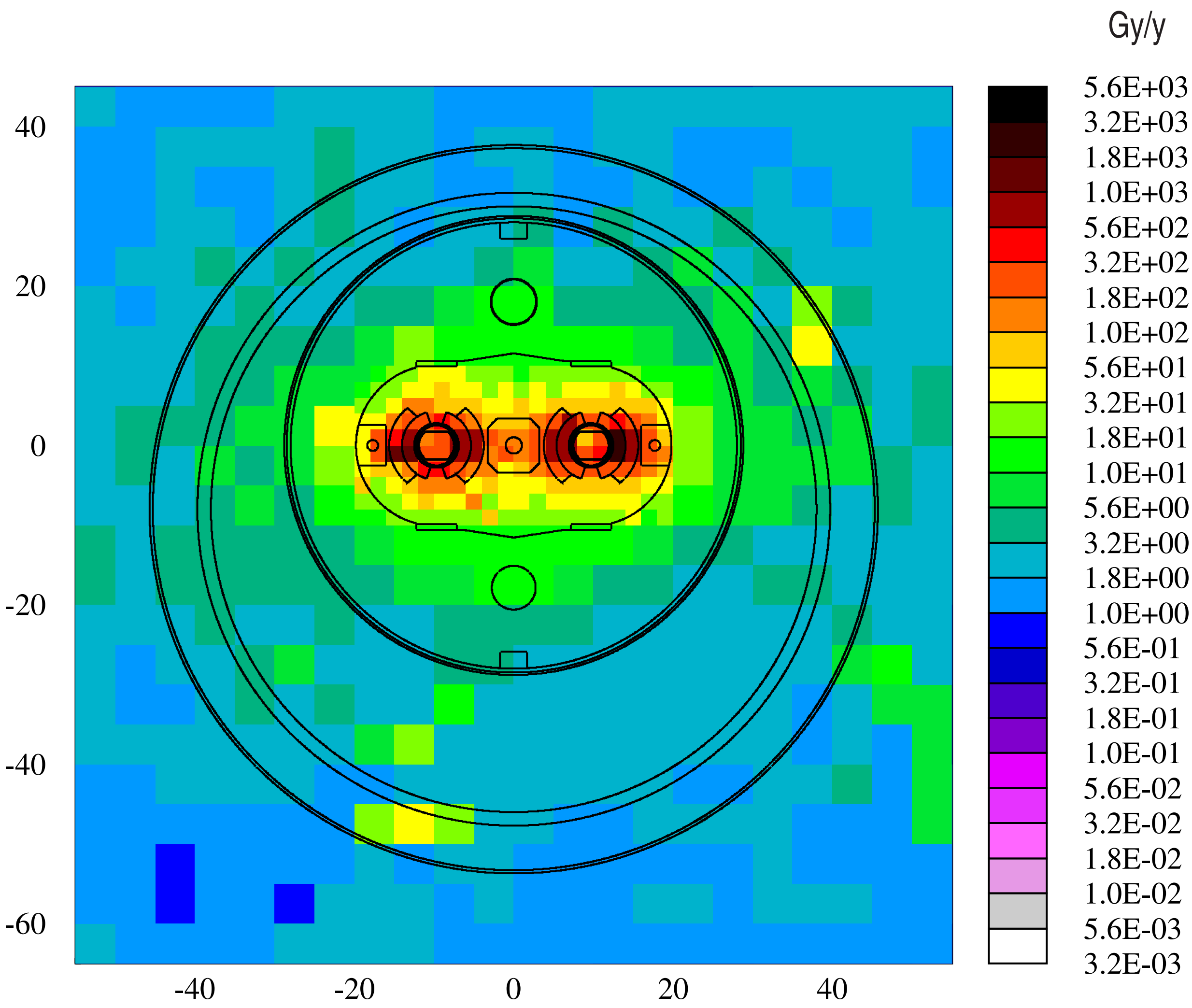

proton losses: 1.65×10^{11} pm^{-1} y^{-1} for 2 beams

Figure 14

Annual dose to MCS corrector and dipole end coils (Q+1)

(50cm longitudinal scoring bin - shaded)

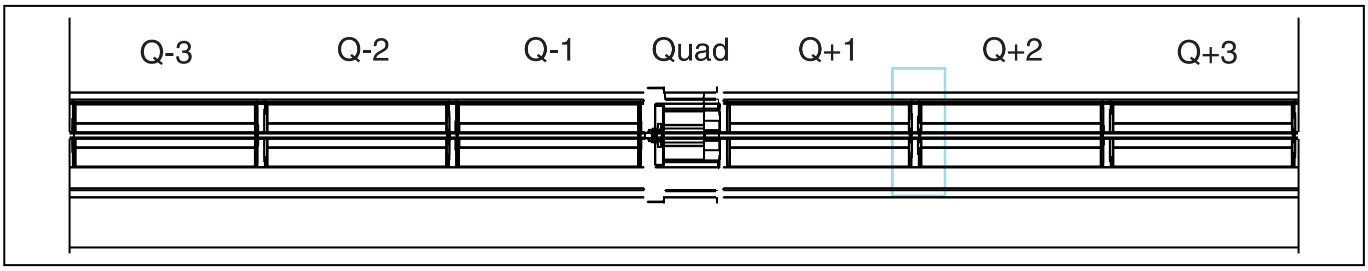

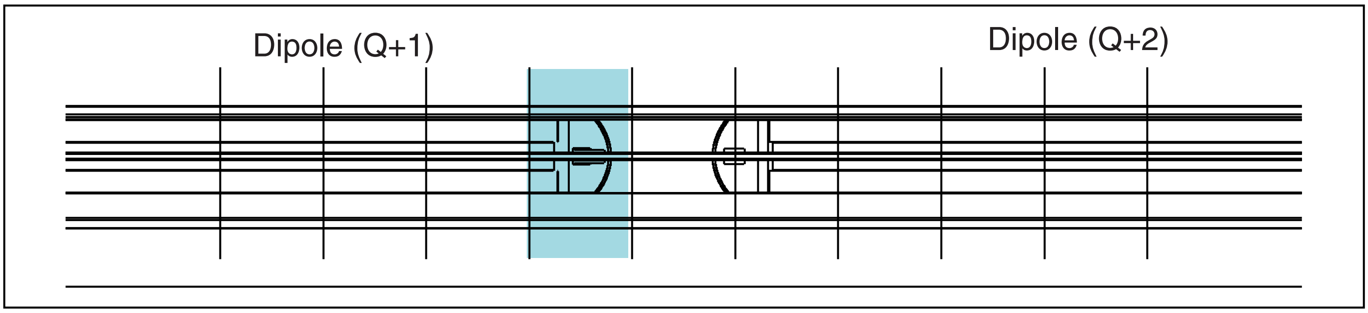

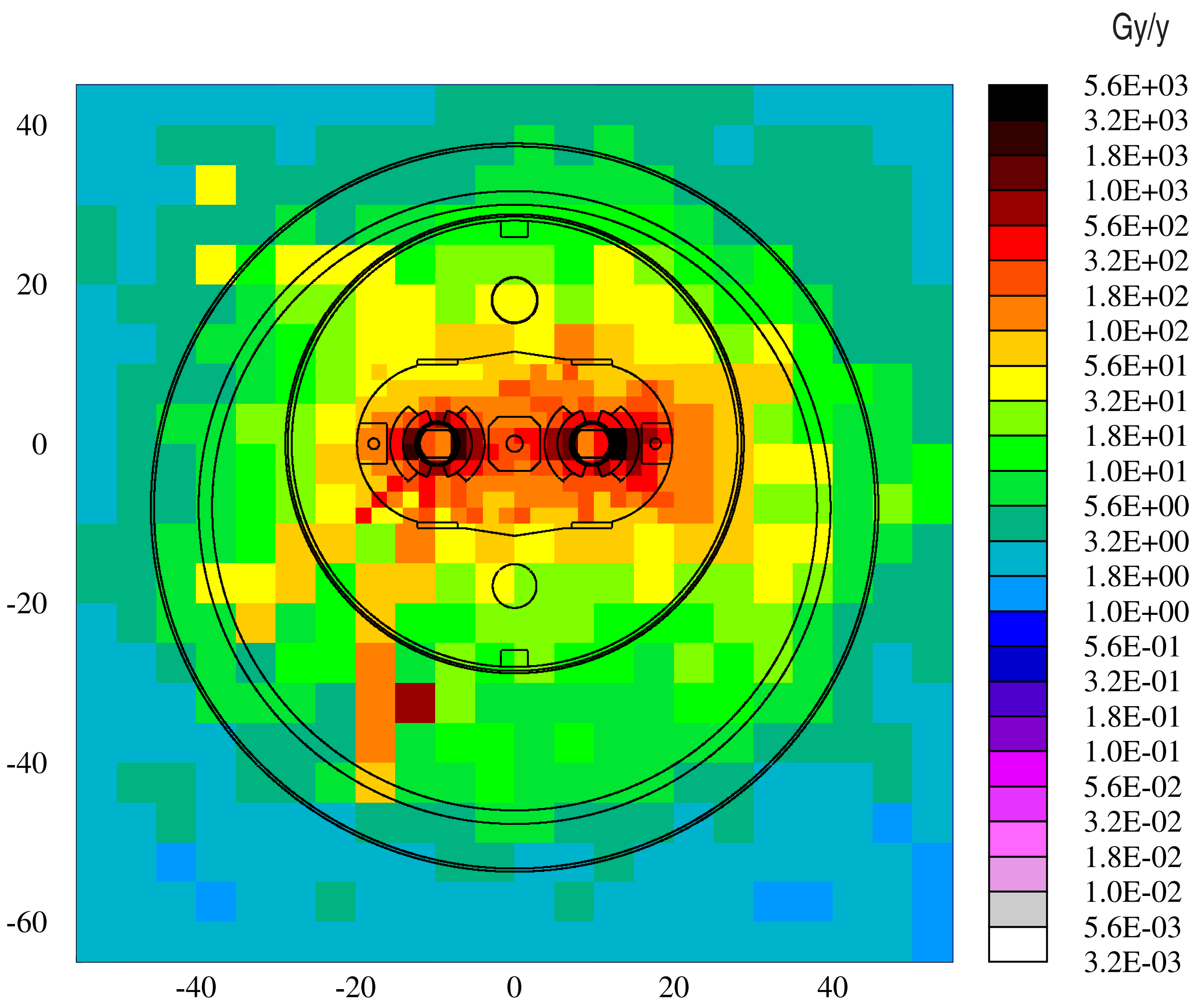

proton losses: 1.65×10^{11} pm^{-1} y^{-1} for 2 beams

Figure 15

Annual dose to decapole corrector and dipole end coils (Q+2)

(50cm longitudinal scoring bin - shaded)

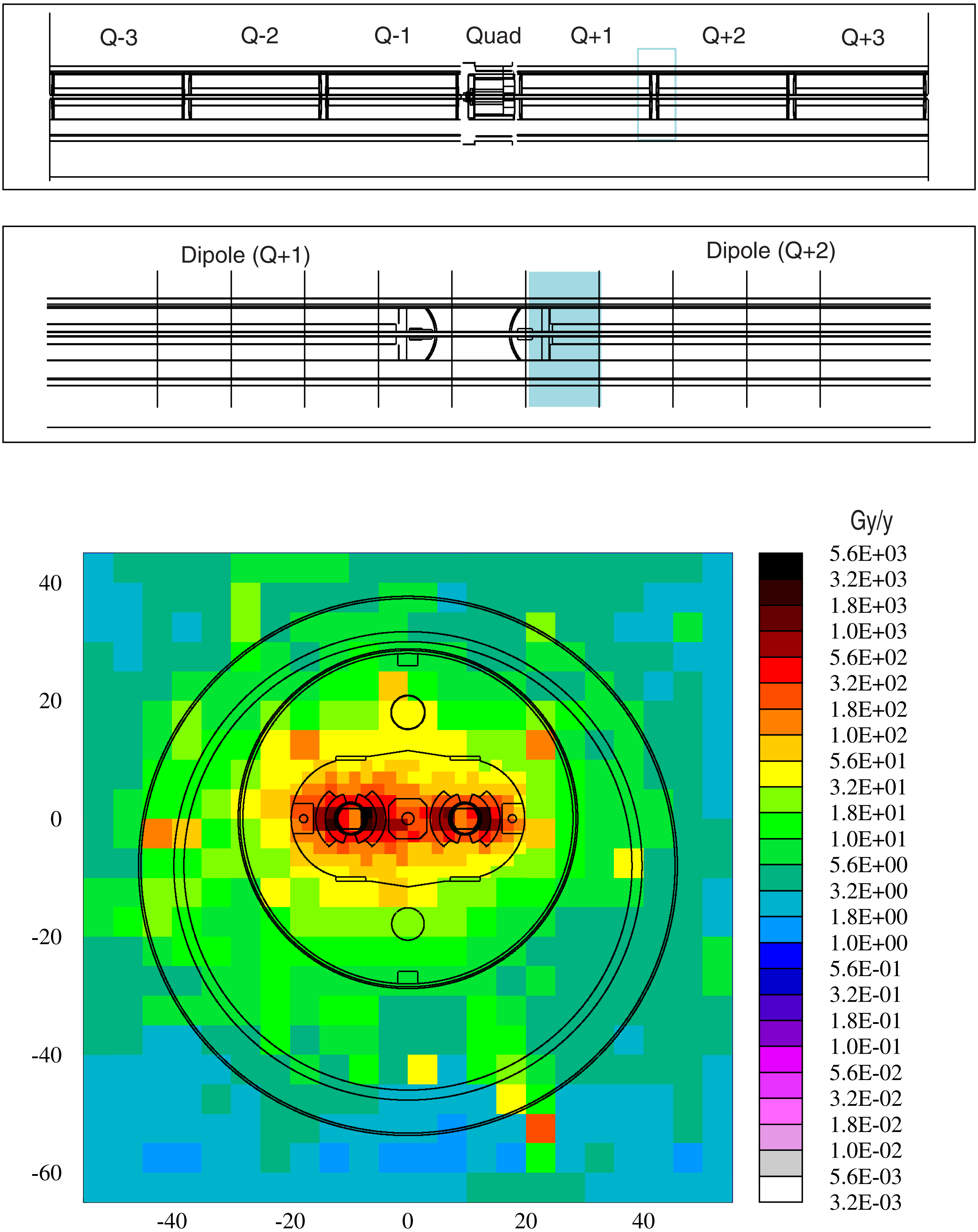

proton losses: 1.65×10^{11} pm^{-1} y^{-1} for 2 beams

Figure 16

Annual dose to dipole end coils and MCS corrector (Q+2)

(50cm longitudinal scoring bin - shaded)

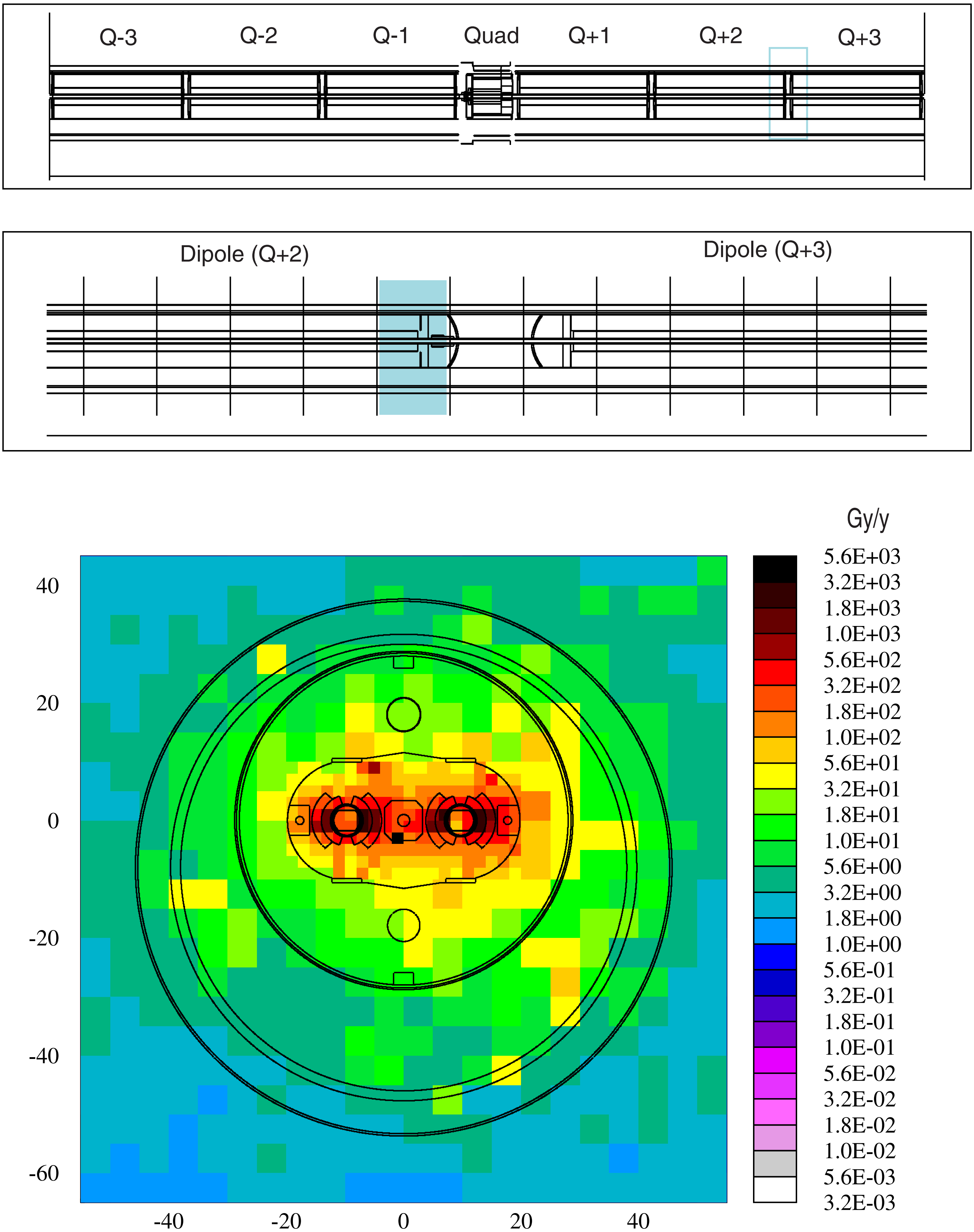

proton losses: 1.65×10^{11} pm^{-1} y^{-1} for 2 beams

Figure 17

Inner regions of LHC arc magnets

Quadrupole

Annual Dose around quadrupole - LHC arcs

Longitudinal cut through quadroupole showing intermagnet gap and area under quadrupole. Doses shown are the average of bins (total width 60cm) about cental point between beamlines.

Longitudinal bins of length = 50cm

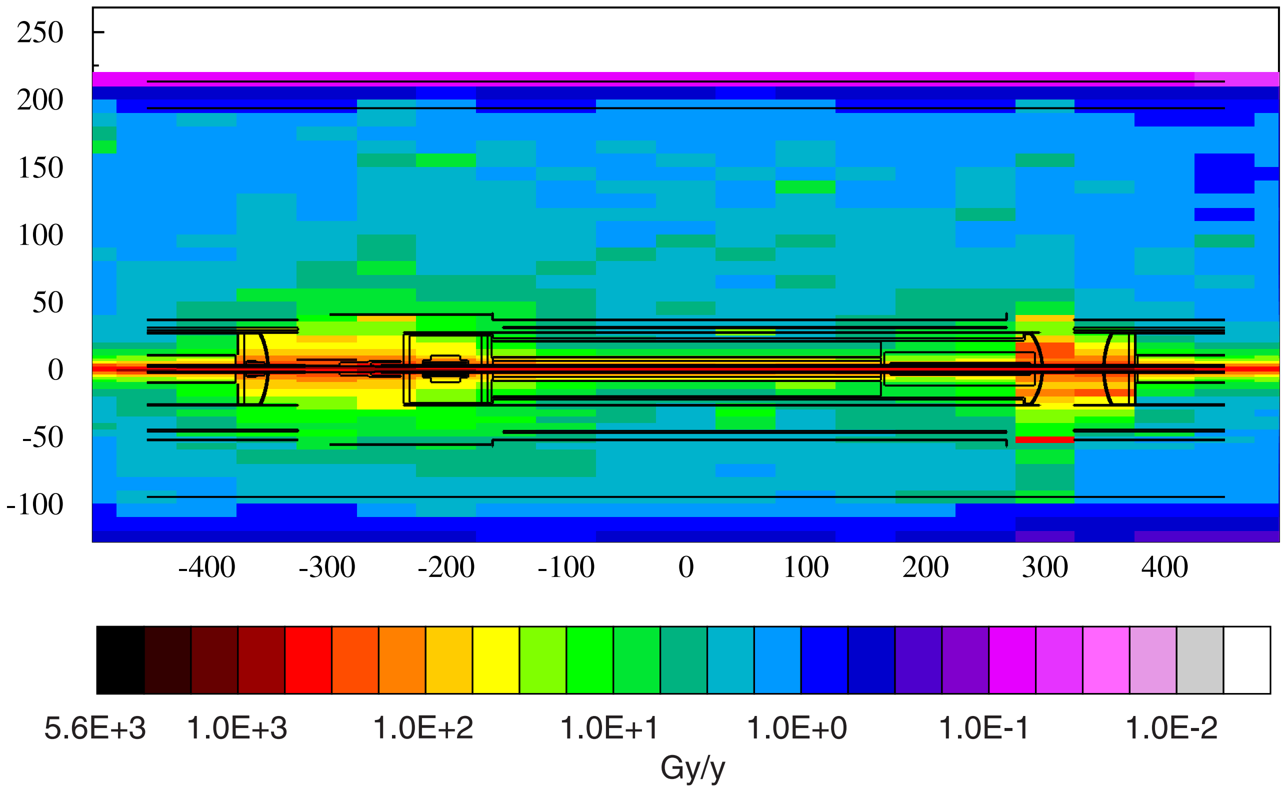

Figure 18

Annual dose to inner region of arc quadrupoles
(averaged over 2.5m of quadrupole coil)

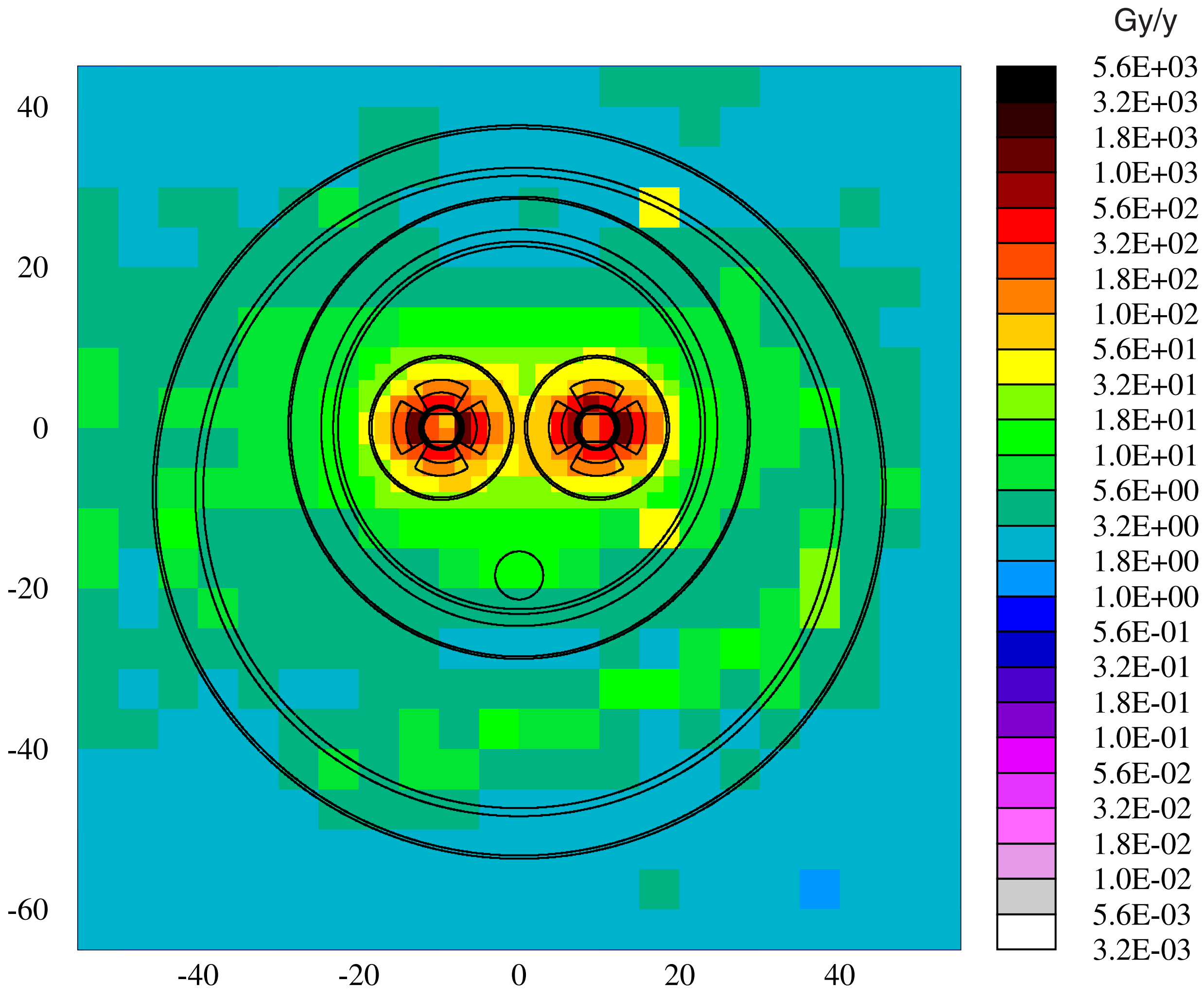

proton losses: $1.65 \times 10^{11} pm^{-1} y^{-1}$ for 2 beams

Figure 19

Annual dose to octupole corrector magnet (MO) in arc quadrupole

(50 cm scoring bin - shaded)

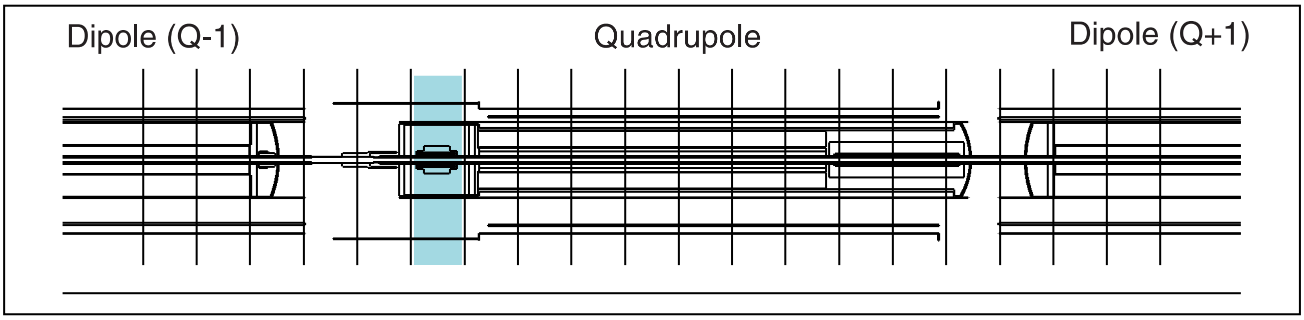

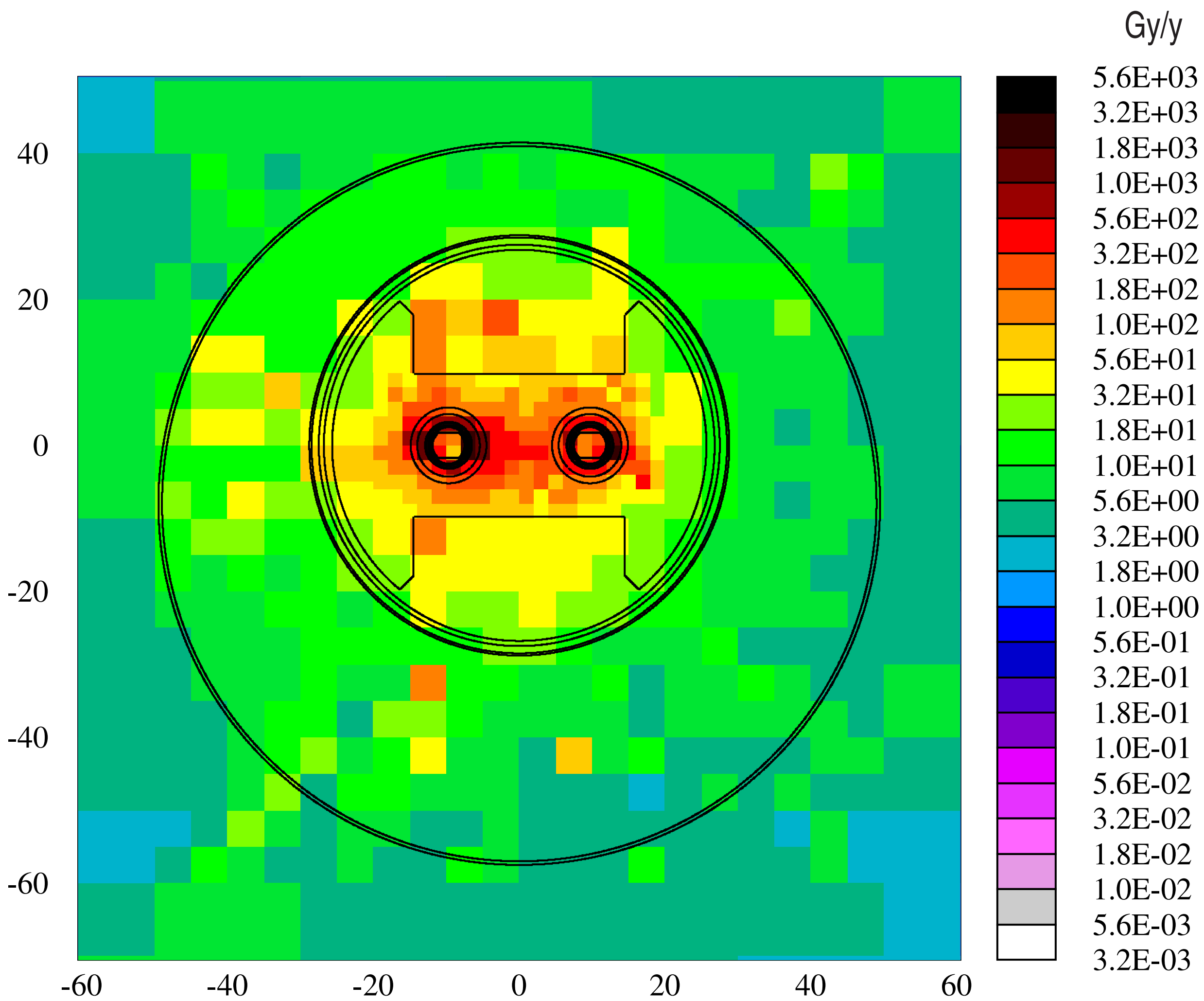

proton losses: 1.65×10^{11} pm^{-1} y^{-1} for 2 beams

Figure 20

Annual dose to quadrupole corrector magnet MSCB

(average over 1m - shaded bins)

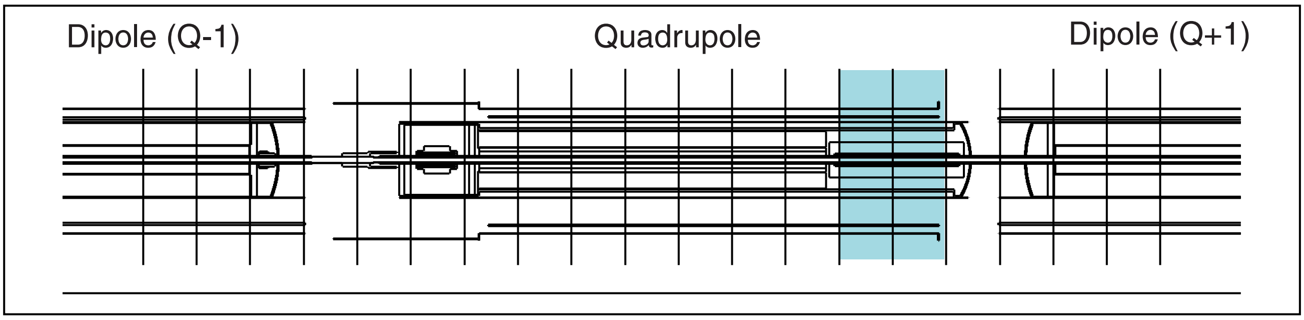

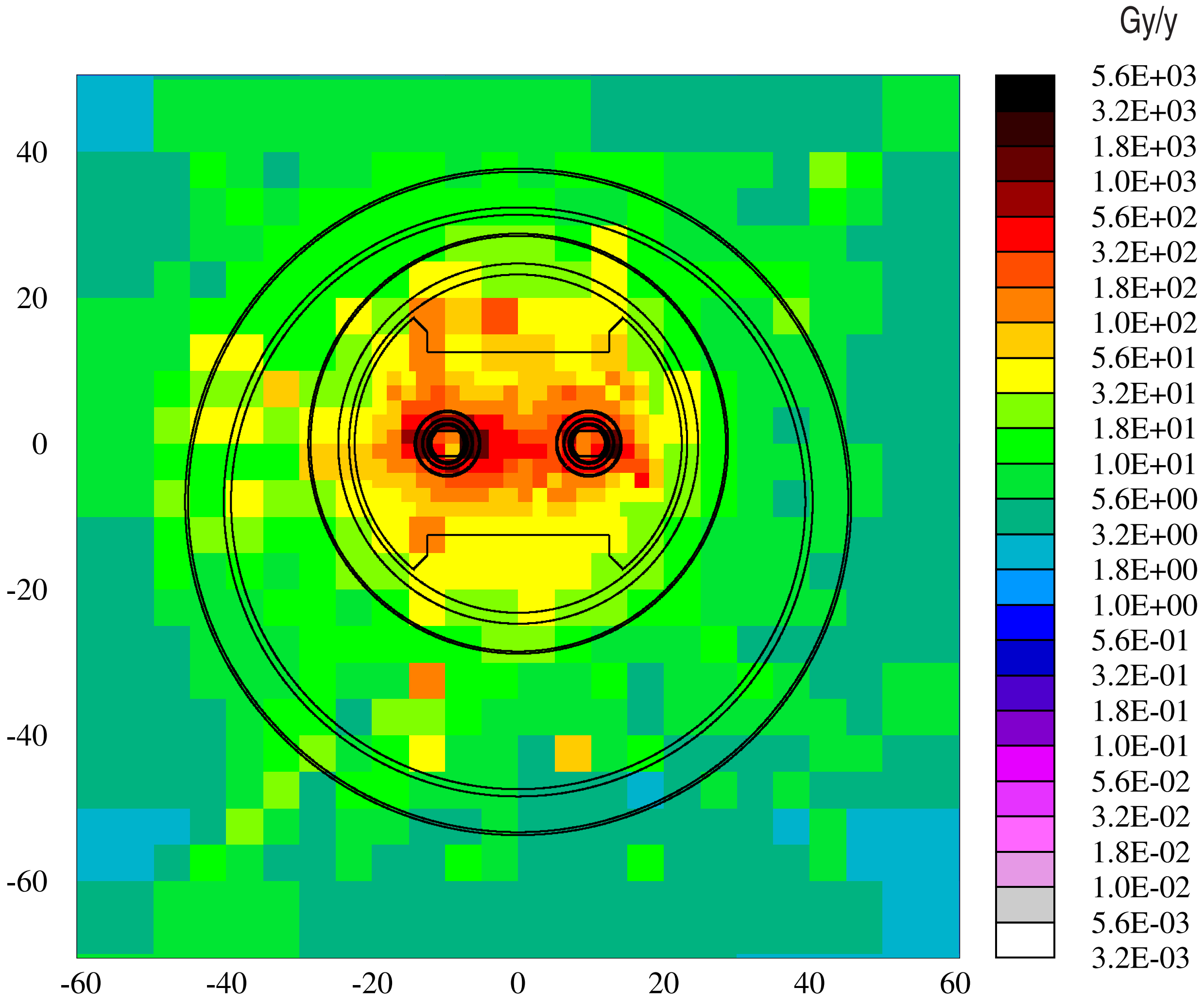

proton losses: 1.65×10^{11} pm^{-1} y^{-1} for 2 beams

Figure 21

Inner regions of LHC arc magnets

Inter-magnet gaps

Annual dose in inter-magnet gap between dipole | quadrupole
(average over 1m - shaded bins)

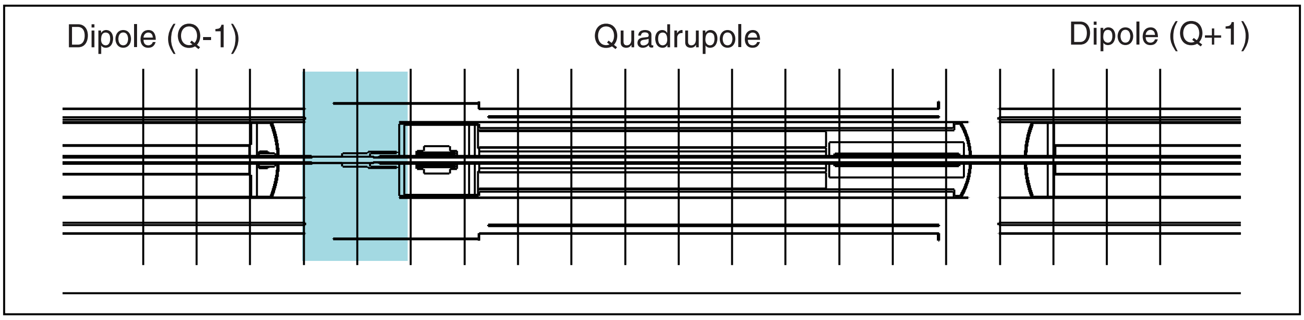

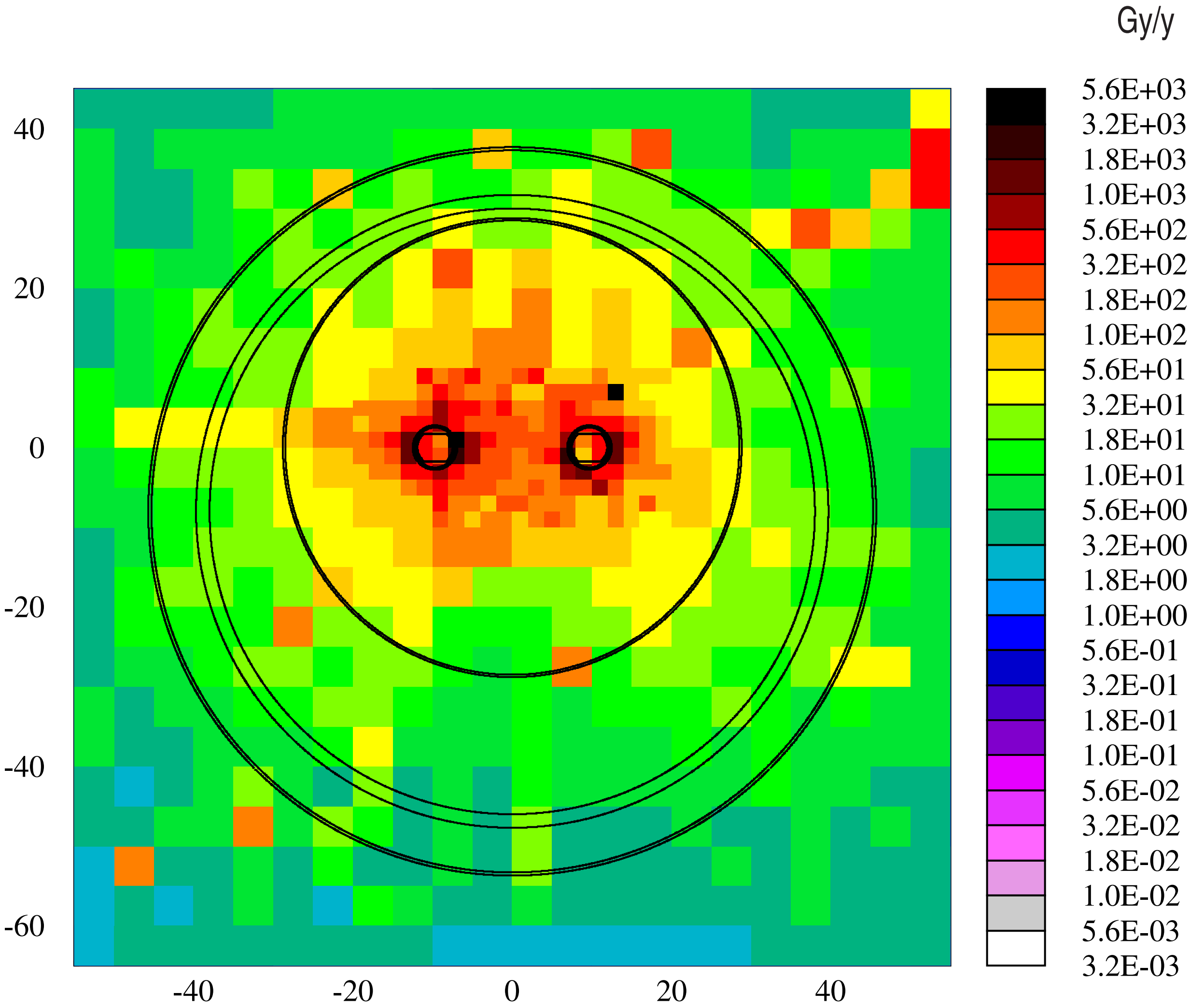

proton losses: 1.65×10^{11} pm^{-1} y^{-1} for 2 beams

Figure 22

Annual dose in inter-magnet gap between dipole | quadrupole

(average over 1m - shaded bins)

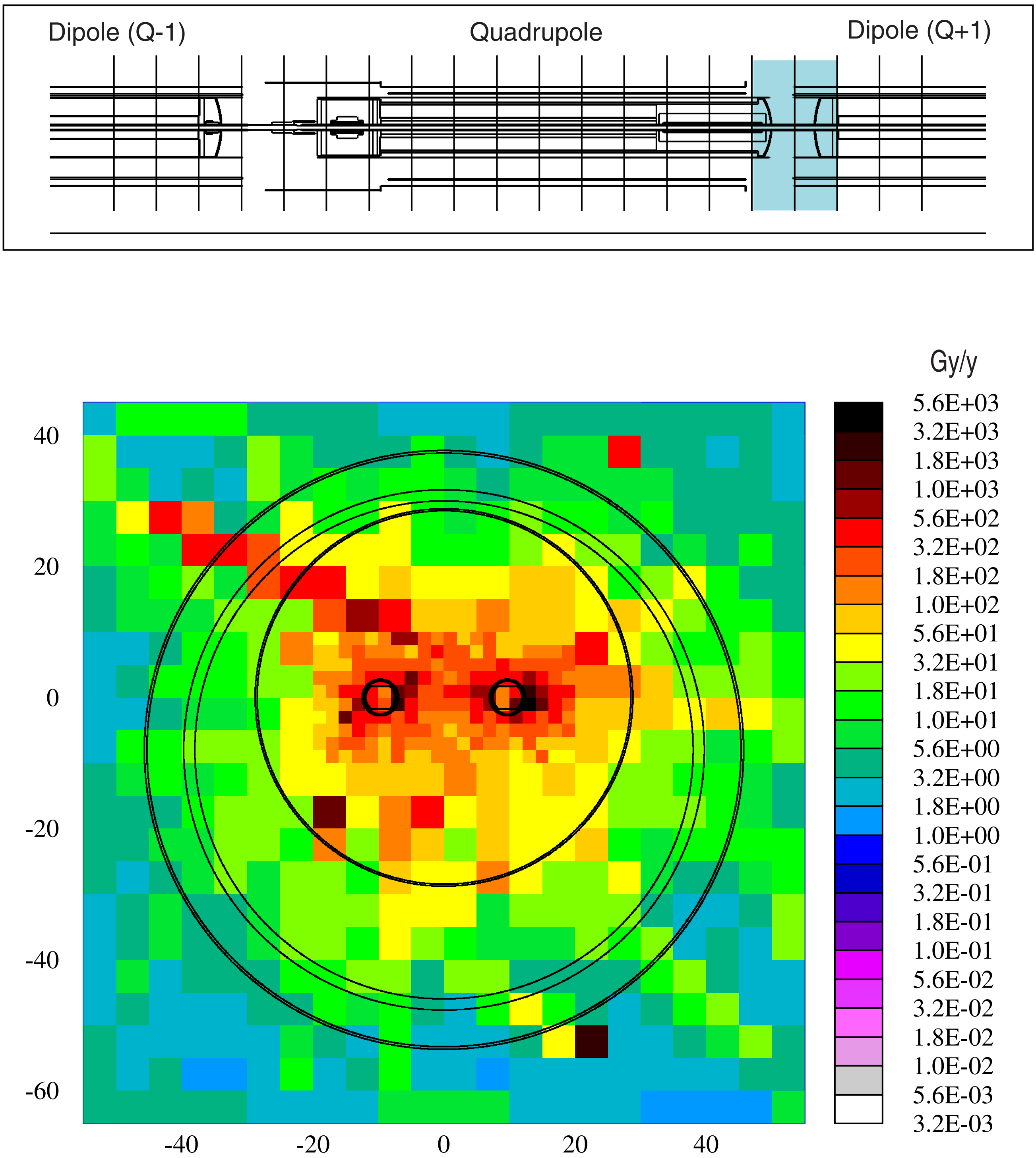

proton losses: 1.65×10^{11} pm^{-1} y^{-1} for 2 beams

Figure 23

Annual dose in dipole - dipole inter-magnet gap

(50cm longitudinal scoring bin - shaded)

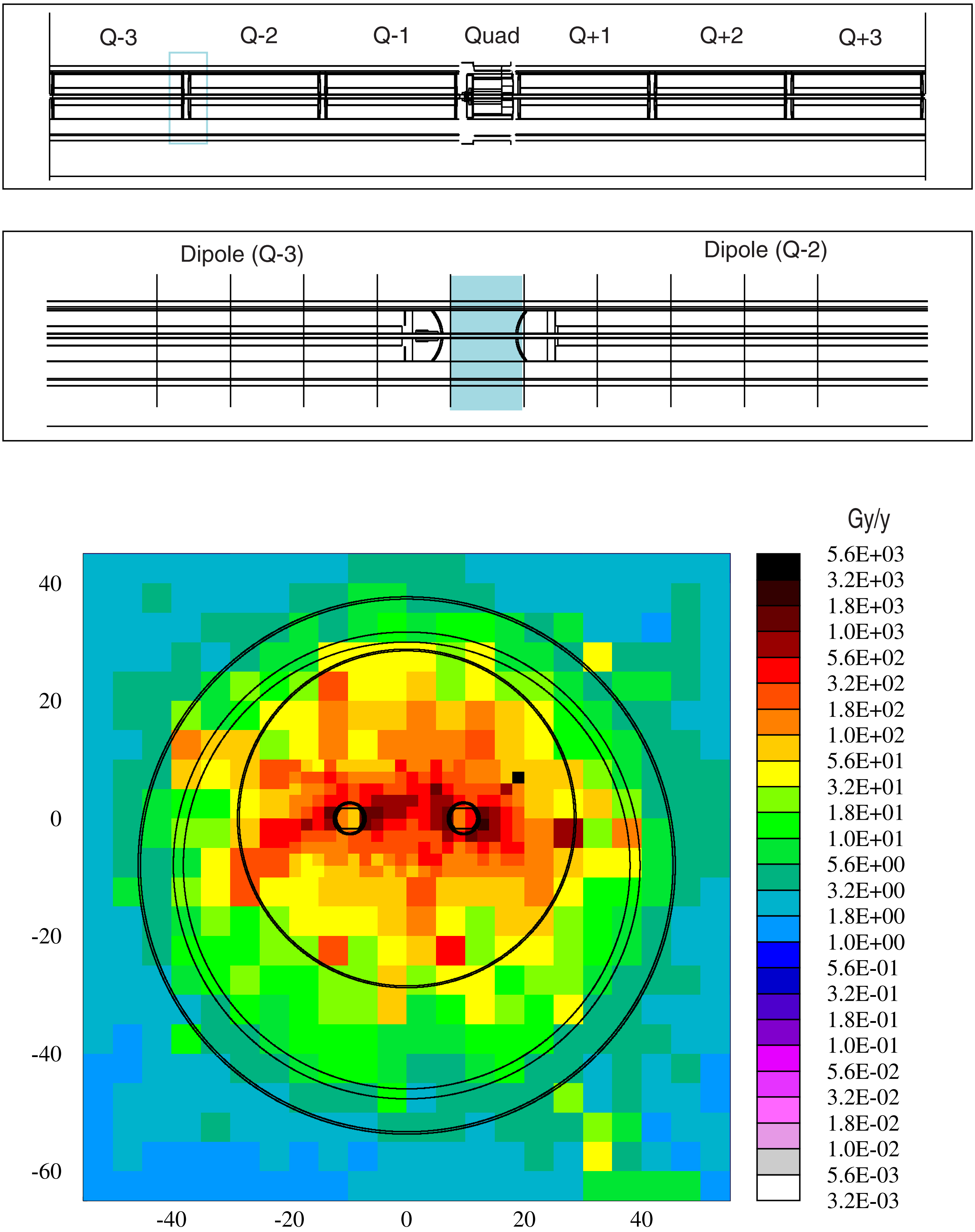

proton losses: 1.65×10^{11} pm^{-1} y^{-1} for 2 beams

Figure 24

Annual dose in dipole - dipole inter-magnet gap

(50cm longitudinal scoring bin - shaded)

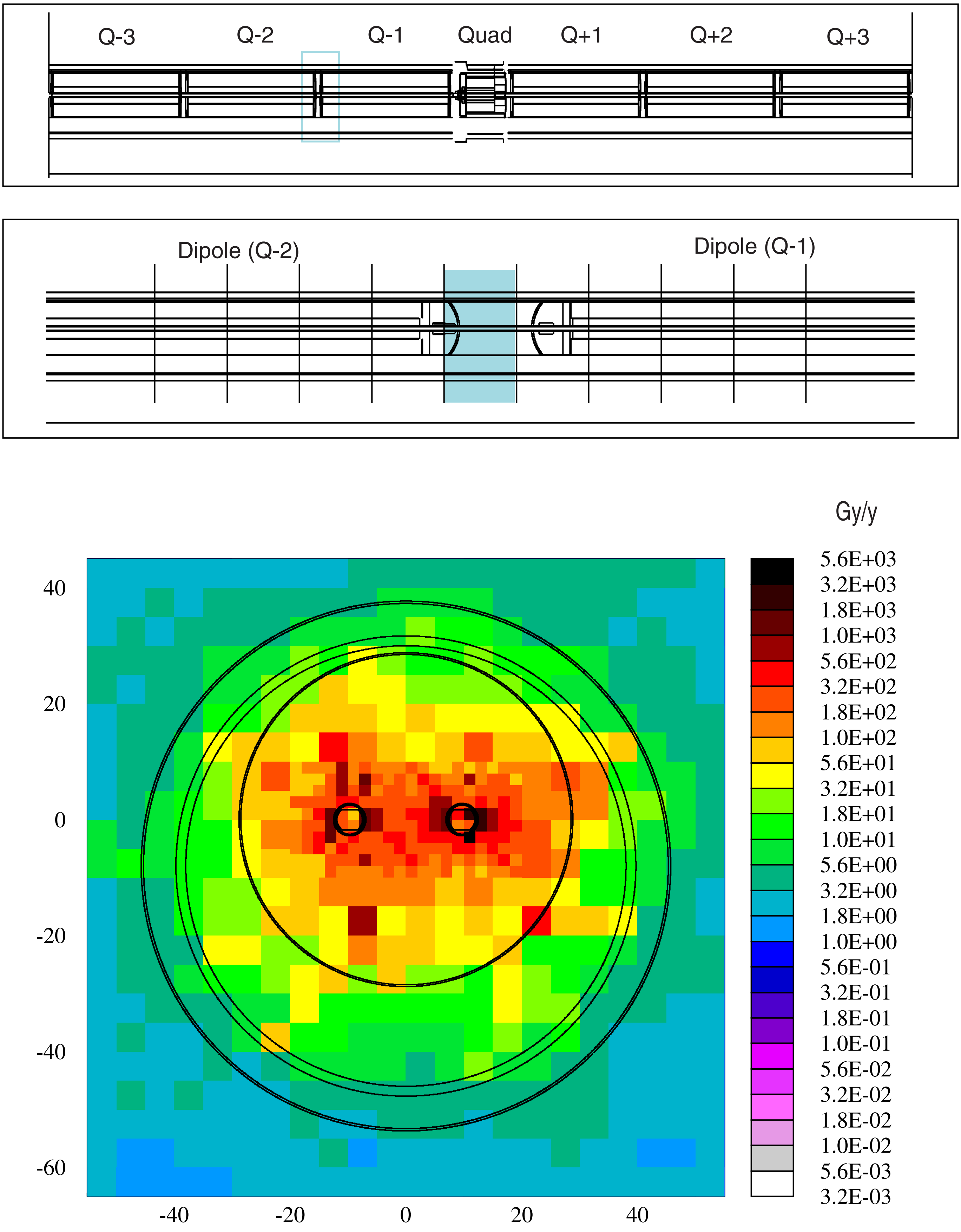

proton losses: 1.65×10^{11} pm^{-1} y^{-1} for 2 beams

Figure 25

Annual dose in dipole - dipole inter-magnet gap

(50cm longitudinal scoring bin - shaded)

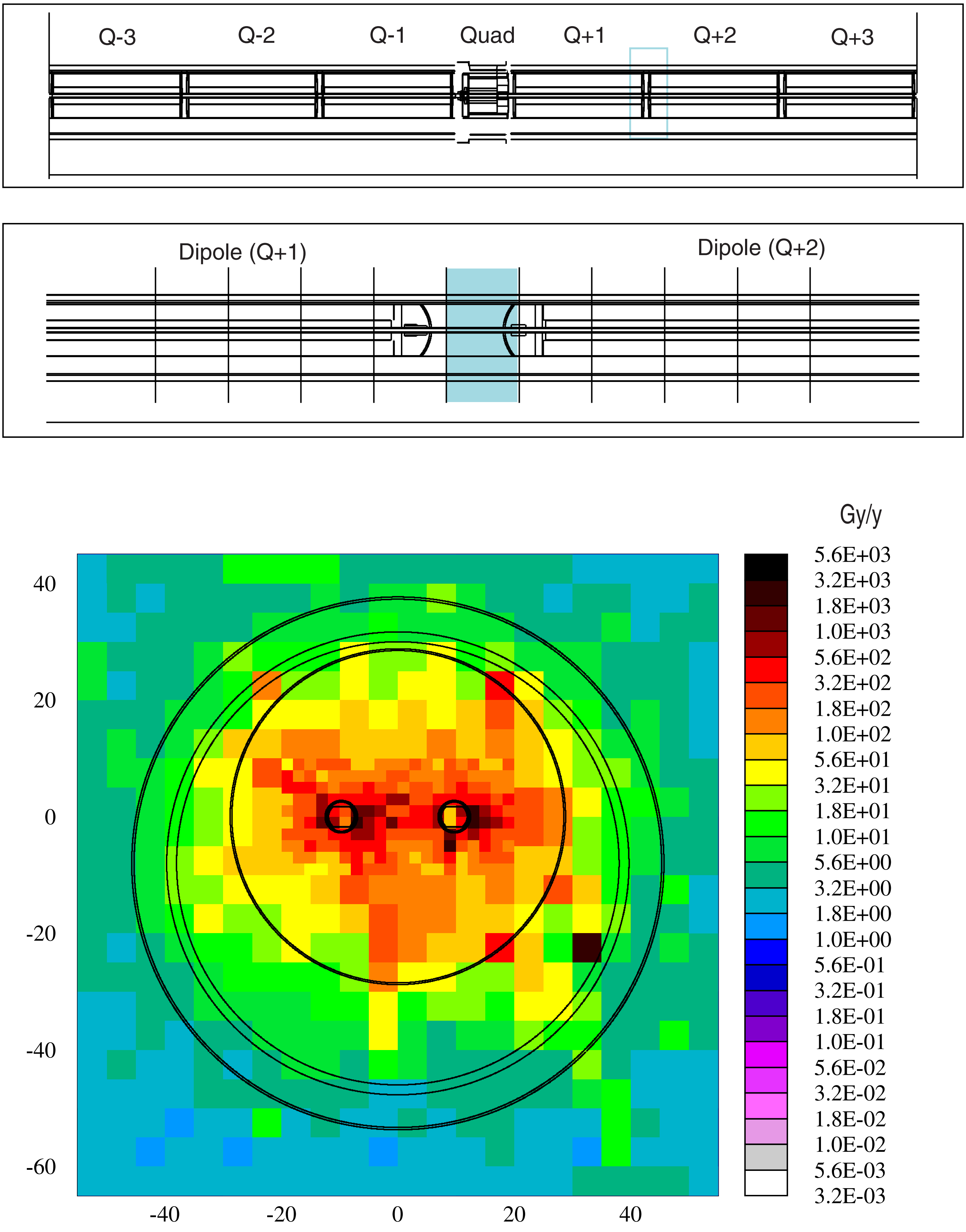

proton losses: 1.65×10^{11} pm^{-1} y^{-1} for 2 beams

Figure 26

Annual dose in dipole - dipole inter-magnet gap

(50cm longitudinal scoring bin - shaded)

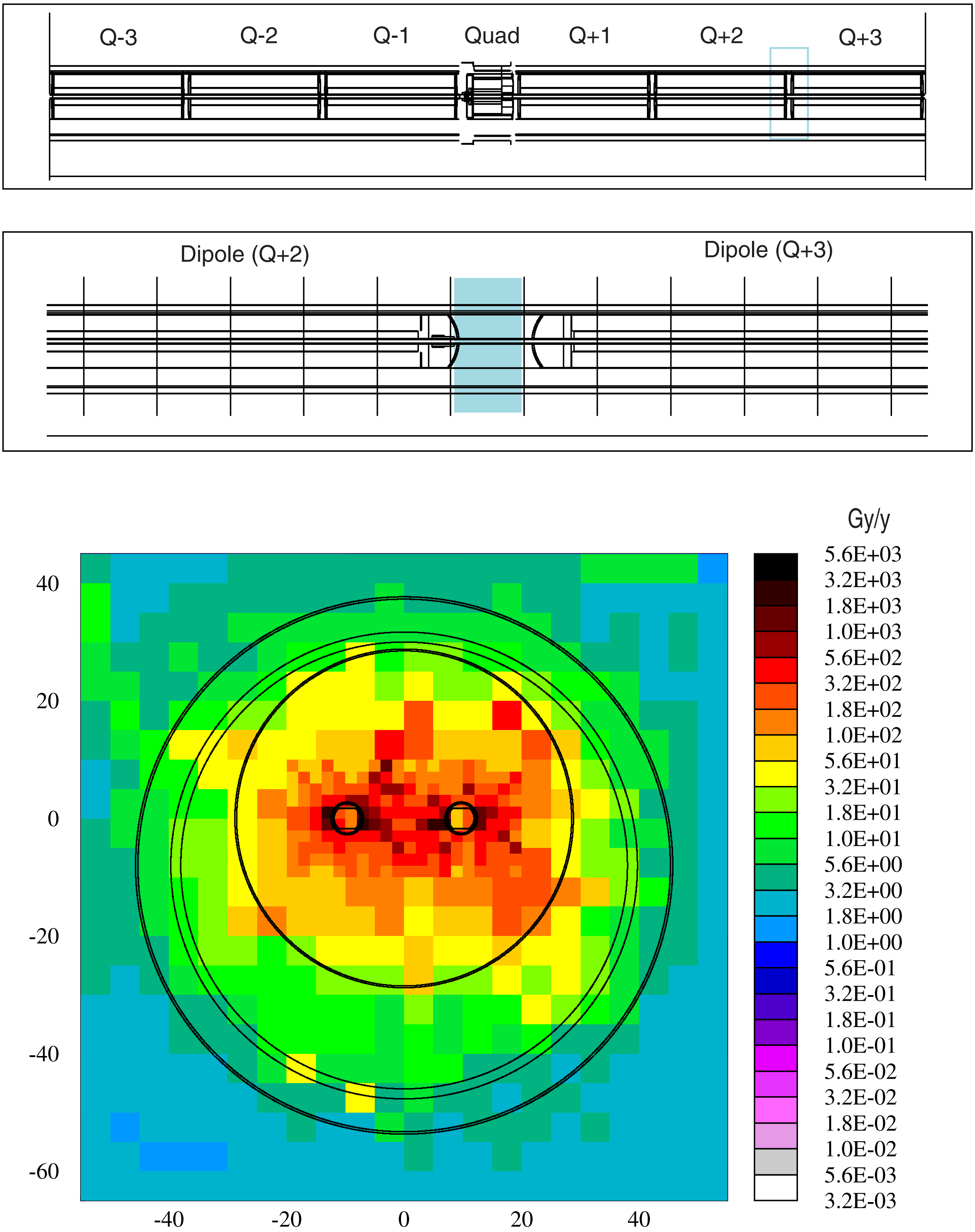

proton losses: 1.65×10^{11} pm^{-1} y^{-1} for 2 beams

Figure 27